

POLITECNICO DI MILANO



Facolta di Ingegneria dei Processi Industriali

Dipartimento di Chimica, Materiali e Ingegneria Chimica "Giulio Natta"

Measurement of Extensional Viscosity of cellulose
Acetate solution using Capillary Breakup
Extensional Rheometry

Relatore:

Prof. Francesco BRIATICO VANGOSA

Student:

Charles Ohene NTI

Mat no. 749812.

A.A. 2011/2012

TABLE OF CONTENTS

1.0 INTRODUCTION.....	4
1.1 BACKGROUND.....	4
1.2 PROBLEM STATEMENT.....	5
1.3 OBJECTIVES	6
1.4 ORGANISATION OF STUDY	6
2.0 LITERATURE REVIEW	7
2.1 RHEOLOGY	7
2.1.1 Newtonian and Non-Newtonian Fluids.....	8
2.1.2 Extensional flow	10
2.1.3 Rheology of Polymer solutions.....	12
2.2 MOLECULAR WEIGHT DETERMINATION	18
2.3 CAPILLARY BREAKUP EXTENSIONAL RHEOMETER (CABER).....	19
2.3.1 Extraction of Viscosity for a Newtonian Fluid.....	22
2.3.2 Apparent Extensional Viscosity.....	24
2.4 CELLULOSE ACETATE	27
2.4.1 Uses of cellulose acetate.....	28
2.4.2 Solubility of cellulose Acetate	28
2.4.3 Structure of cellulose derivatives in solution.....	30
2.4.4 Structural characterization of cellulose acetate	31
2.4.5 Rheology of Cellulose Acetate Solution.....	32
2.4.5 Thermal properties	35
2.5 ELECTRO SPINNING	37
3.0 METHODOLOGY.....	39
3.1 MATERIAL CHOICE AND SAMPLE PREPARATION.....	39
3.2 EXPERIMENTAL SET UP	40
3.2.1 Capillary Breakup Extensional Rheometer (CaBER)	40
3.2.2 Shear Rheometer	44
3.2.3 Video Recording.....	44

3.3 DATA ANALYSIS.....	44
3.3.1 Determination of D_1 and D_0	44
3.3.2 Apparent Viscosity determination	48
4.0 RESULTS AND DISCUSSIONS	51
4.1 DIAMETER VERSUS TIME.....	51
4.2 EFFECT OF TEMPERATURE	53
4.2.1. Apparent Extensional Viscosity.....	53
4.2.2 Time to Break up	57
4.3 EFFECT OF CONCENTRATION.....	60
4.3.1 Time to Break up	60
4.3.2 Steady State Extensional Viscosity	62
4.4 TIME TO BREAK UP AND STEADY STATE EXTENSIONAL VISCOSITY	65
5.0 CONCLUSION.....	69
6.0 REFERENCES	70
7.0 APPENDIX.....	73
7.1 APPENDIX 1	73
7.2 APPENDIX 2.....	76
7.3 APPENDIX 3.....	78
7.4 APPENDIX 4.....	81

1.0 Introduction

1.1 *Background*

Cellulose acetate finds many uses in engineering and industry, therefore successful characterization of cellulose acetate solution is useful for many industrial and engineering applications. Among other applications, cellulose acetate in methanol have been successfully electro spun and the electro spun fibers shown different morphology with concentration, and thus finding the linkage between solution properties and electrospinning is of importance to industry and research community.

Investigating the rheological behavior of cellulose acetate solutions in conditions close to those used in electrospinning with the goal of finding relationship between the solution rheology and its spinnability defined as the ability to form a continuous jet that is stable against breakup into droplets, in the presence of an electric field [19]. To achieve this objective, we resulted to filament breakup rheometry. This work seeks to find this relationship as well as the effect of other variables on the measurement of extensional viscosity using CaBER.

Filament breakup studies using Capillary Breakup Extensional Rheometer (CaBER) provide a low cost approach to the measurement of effective extensional properties, and this can be performed with low viscosity polymer solutions. By monitoring the dynamics of breakup of a fluid filament following a short rapid extensional deformation, one can obtain information about the relaxation time spectrum, the extent of non-Newtonian behaviour and the time to breakup for the fluid. The latter parameter is of particular value to batch filling applications and also to continuous processes involving free surfaces such as spraying or atomization, inkjet printing, coating flows and spinning [11] The use of CaBER (Capillary Break up Extensional rheometer) for the characterization of solution to be electro spun stand from the fact that electro spinning is an extensional flow process and the effect of elasticity and

surface tension are important and they are the dominant factors in the drainage of a fluid column just like in the CaBER.

The extensional rheological properties of a polymer solution can be extracted by observation of the evolution of a thin fluid of the solution under the combined action of viscous, elastic and capillary forces. In the CaBER instrument, the sample is placed between two plates of known diameters then an exponential elongation is imposed to the fluid column, after the end of the deformation step the evolution of the midpoint diameter is observed. The system is allowed to select its own dynamics so that viscous, elastic, gravitational and capillary forces balance each other [2]. In this case as the tensile force along the fluid column is not measured one needs to understand the deformation mechanism the system selects and why it selects these particular ones in order to be able to extract material parameters like viscosity and relaxation time. [2]

Electrospun fibers have potential applications in nanocomposites, biomedical engineering, protective clothing, sensors, magneto-responsive fibers and superhydrophobic membranes. Also, the performance of the resulting material (product) has been shown to depend strongly on fiber morphology. It is also said that the spinnability of a polymer solution also depends on the elasticity of the solution and experiments show that lack of elasticity prevents the formation of continuous fibers but instead forms droplets or necklace-like structures called “beads-on-strings”. [7]

1.2 Problem Statement

The main concerns are to be able to extract useful material parameters of cellulose acetate solution from CaBER experiments and be able to link them to their processability, for example to be able to predict whether a solution of cellulose acetate can produce a very good morphology of the fibers when spun.

Three samples of Cellulose acetate in a solution of methanol (75% dichloromethane and 25% methanol) are tested in CaBER (Capillary Break-up Extensional Rheometer) at different temperatures and solution concentrations. Extraction of useful rheological properties from the CaBER instrument and also the effect of temperature on the test samples will be investigated.

1.3 Objectives

1. To characterize solution of cellulose acetate in Methanol using CaBER (Capillary Break up Extensional Rheometer)
2. Investigate the effect of evaporation on test samples.
3. To determine the relationship between rheological properties and spinnability of cellulose acetate solution.

1.4 Organisation of Study

In this study the background, problem statement and objectives forms chapter one of the project. Chapter two contains the literature review of the whole project. Chapter three will contain the methodology and Chapter four concerns the results and discussion while chapter five will be the conclusion and recommendation.

2.0 Literature Review

2.1 Rheology

Rheology is defined as the study of the flow and deformation of materials, with special emphasis being usually placed on the flow which may not be limited to fluids but also soft matter. The term Rheology was first used by E. C. Bingham and M. Reiner in 1929 [6]. Rheology deals with the flow properties of liquids. Rheometry describes methods and devices used to measure these flow properties of the fluid. In describing the flow, it is important to know the relative motion of the element of the fluid to each other; the type of flow and the deformation become characteristic of that material.

When a force is applied to a material and the deformation experienced by it reverts to its original position after the removal of the force; we have elastic behavior of the liquid or material. This is the behaviour of real solids which obey the Hooke's law. There is full recovery of the energy input. On the other hand when the deformation remains when the applied force is removed and the material remains in that shape, we have viscous behaviour; the energy involved is used in doing work, i.e. in causing the material to flow. Most materials do not exhibit pure elastic or viscous behavior but rather a mixture of the two and are known as viscoelastic materials.

There are two basic kinds of flow with relative movement of adjacent particles of liquid; they are called shear and extensional flows. In shear flows liquid elements flow over or past each other, while in extensional flow adjacent elements flow towards or away from each other [4]. Figure 2.1 illustrates a simple shear flow in which a force \mathbf{F} is applied to a surface \mathbf{A} on the top movable plate. The velocity of the plate is \mathbf{v} and the distance between the plates is \mathbf{h} . [6]

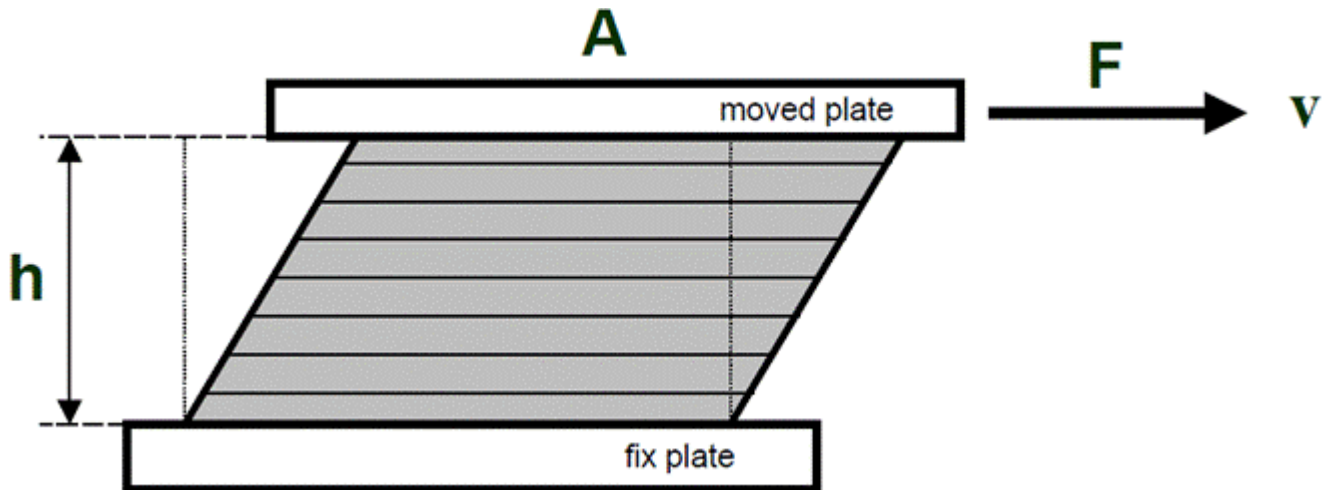


Figure 2.1 schematic of a simple shear flow.

The shear stress (τ) is defined as F/A , the shear rate ($\dot{\gamma}$) is dv/dh . The relationship between the shear stress and shear strain is given by equation 1 which is often called the Newton law of viscosity.

$$\tau = \eta(\dot{\gamma}) \quad (1)$$

The resistance to flow of these elements when a force is applied to it is termed viscosity (η) which is an important property when it comes to studying rheology defined mathematically as the shear stress over the shear rate from equation 1. It often describes the internal friction among particles of the fluid during flow. For example a liquid with low viscosity will easily flow because there is less resistance while one with high viscosity will have difficulty in flowing. Often this property plays very important role in our day to day activities as well as in many industrial applications. For example; Ink in biros and roller-ball pens that must have a low viscosity as it is being dispensed through the high-shear-rate roller-ball mechanism. However, when the ink is sitting on the writing surface, its viscosity must be high to stop it spreading far. [4]

2.1.1 Newtonian and Non-Newtonian Fluids

Newtonian fluids are those that their viscosity does not change with strain rate. Their viscosity remains constant with varying strain rate but can vary with other factors like temperature, pressure etc. There is

a linear relationship between shear stress and shear rate and the constant of proportionality is the viscosity (equation 1). A typical example is water.

Non-Newtonian fluids have their viscosity changing with strain rate and the shear stress and strain rate relationship is non-linear or does not pass through the origin that is does not follow the Newtonian law (equation 1). Depending on the relation between the shear stress and strain, the fluid can be named as follows;

Those that have their viscosities decrease with increasing strain rate are known as shear thinning. For polymer solution, at low shear rates, the viscosity is independent on shear rate and this value is known as the zero-shear rate viscosity. Also, at very high shear rates there is another plateau which is the infinite viscosity. In-between these strain rate extremes, the viscosity of a shear thinning decreases with increasing strain rate. While those showing an increase in viscosity with strain rate are shear thickening, these also exhibits some limiting values at low and very high (or infinite) shear rates. When a limiting value of the strain rate is needed to cause flow of the fluid we have Bingham plastic fluid whose shear stress-strain rate graph is linear but does not pass through the origin. Figure 2.2 shows the various fluid types discussed above. Examples of Non-Newtonian fluids are; polymer solutions, suspensions, toothpaste etc.

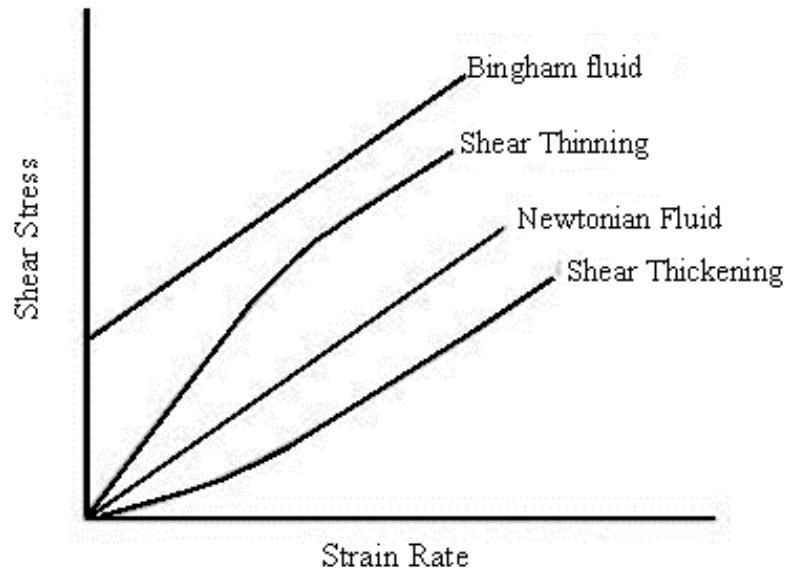


Figure 2.2 Schematic representation of stress – strain behaviour of different fluids

There are some non-Newtonian fluids in which the behavior is also time dependent, that is at constant shear rate, the stress tends to decrease or increase with time. When the viscosity decreases with time we have Thixotropic behaviour and when it increases with time; Rheopectic behaviour.[5]

2.1.2 Extensional flow

In extensional flow the elements of a fluid are stretched out or squeezed down rather than sheared. The particles turn to deform rather than shear as the fluid experiences a stretching or elongation as opposed to shearing. The forms of extensional flows are uniaxial, biaxial and planar as shown schematically in Figure 2.3 [5]. Examples of phenomenon in which extensional flow occurs are; spinning, break-up of liquid jets, droplet break-up, atomization and spraying. Others include; film blowing injection moulding and extrusion. [5]

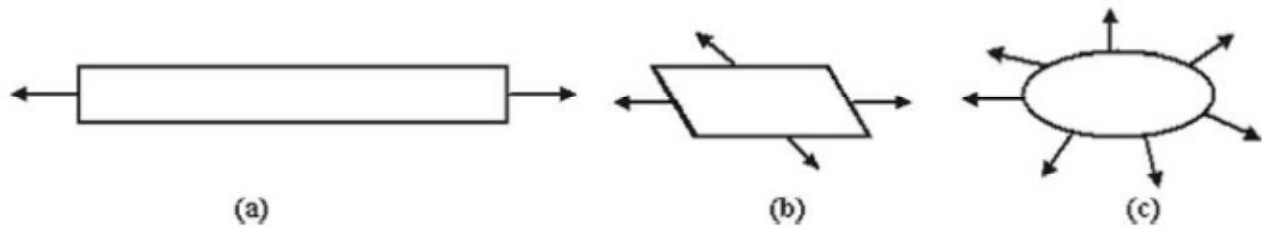


Figure 2.3 Schematic representation of uniaxial (a), biaxial (b) and planar (c) extension

The deformation of the particles of the fluid causes an increase in the viscosity of the fluid. In a shear flow the particles turn to align in the flow axis resulting in minimum resistance while in extensional flow the particles still align with the flow axis but with maximum resistance because the fluid around the particles tries to deform the particles.

The increase in resistance causes an increase in viscosity and so extensional viscosity is greater than shear viscosity. The mechanism that results in extensional viscosity being greater than shear viscosity are; aligning particles with the flow results in maximum resistance, strong interaction of extensional flows and network dynamics and coil-stretch transition giving very long aligned particles [4].

Mathematically the extensional viscosity of Newtonian fluids is related to the shear viscosity by equation 2 [4]. Example of extensional flow is the flow in a tube with changing diameter which is illustrated schematically in figure 2.4.

$$\eta_e = 3\eta \quad (2)$$

η_e - Extensional viscosity and η - shear viscosity

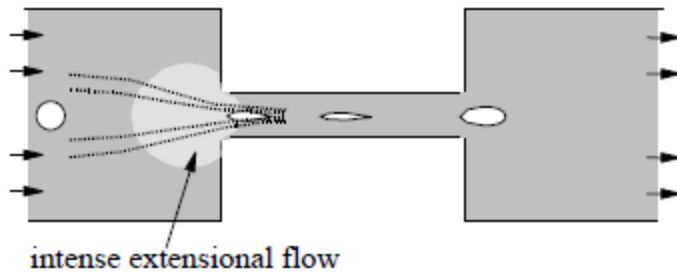


Figure 2.4 Illustration of the deformation of a liquid droplet from a high to small diameter as it experiences extensional flow [4]

2.1.3 Rheology of Polymer solutions

The viscosity of polymer solutions does not only depend on shear rate and temperature and in some extreme cases pressure but also on the molecular weight distribution, degree of branching and the concentration. For polymer solutions, the solvent properties are also important since the quality of the solvent can vary for organic liquids from ‘good’ to ‘bad’, eventually having effects on the viscosity.

The shape of the macromolecule in solution depends on the type of the chains and the solvent; polymers can be coils or string like. They can also be either linear or branched. At a low concentration linear coils are isolated and non-interacting, and they take up an approximate spherical shape, which is dictated by thermodynamics. The shape of the molecule in solution determines the space occupied and this further affects the behavior of the solution. During the application of a shear force to a solution of low concentration, these spheres tends to become ellipses aligned along the direction of the force and at very high shear rates, they can be stretched out in the direction of the force (complete alignment or rod-like). The dependence of viscosity of the chain configuration can be seen in figure 2.5 where the viscosity decreases as the chains align to the flow [4]. This is due to high resistance to flow of spherical particles than rod-like particle given rise to a decrease in the viscosity with high strain rates.

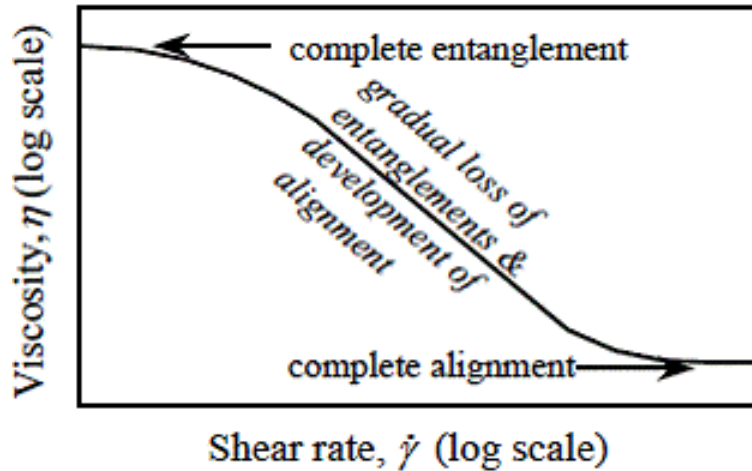


Figure 2.5 The flow curve for a polymer solution showing the two extremes of complete entanglement and complete alignment.[4]

The dependence of molecular weight on shear viscosity is a rise in the shear viscosity with molecular weight through increase in the segment density. The dependence on intrinsic viscosity of polymer solution is given by Mark-Houwink equation shown in equation 3 [4].

$$[\eta] = KM^\alpha \quad (3)$$

M is the molecular weight and K and α are constants for particular kinds of polymers, for instance α varies from 0.5 for a random coil to 2 for a rigid rod. The presence of solvent in solution greatly affects the rheology of solution as against that of polymer melts which is made up of only the chains without the solvent. The effect is as a result of the interaction between the polymer chains and the particles of the solvent.

The intrinsic viscosity $[\eta]$ can be defined as the contribution of solute to the viscosity of the solution. It is expressed as the limiting value of the reduced viscosity η_{red} at zero concentration (4c). The reduced viscosity is the ratio of the specific viscosity (η_{sp}) to the concentration of the solution (4b), while the specific viscosity is the ratio of the polymer viscosity to that of the solvent (4a). The intrinsic viscosity

is measured in reciprocal of density (ml/g) and it represents the volume the polymer will occupy in solution [3].

$$\eta_{sp} = \frac{\eta_2}{\eta_1} = \frac{\eta - \eta_1}{\eta_1} = \frac{\eta}{\eta_1} - 1 = \eta_{rel} - 1 \quad (4a)$$

$$\eta_{red} = \frac{\eta_{sp}}{c} \quad (4b)$$

$$[\eta] = \lim_{c \rightarrow 0} \eta_{red} \quad (4c)$$

where η_{rel} is the relative viscosity, η_1 the solvent viscosity, η_2 the solute (polymer) viscosity, η is the viscosity of the solution ($\eta_1 + \eta_2$), c solution concentration

As the concentration of the solution increase there is interaction between the polymer coils and the behavior changes. The concentration at which these interaction become important is called the critical overlap concentration (c^*) and the concentration range, where the overlap interaction is important is $1 < c[\eta] < 10$ which is dependent on the volume of the molecules. The effect of concentration on zero-shear viscosity in figure 2.6 shows a change in gradient through the critical concentration (c^*).

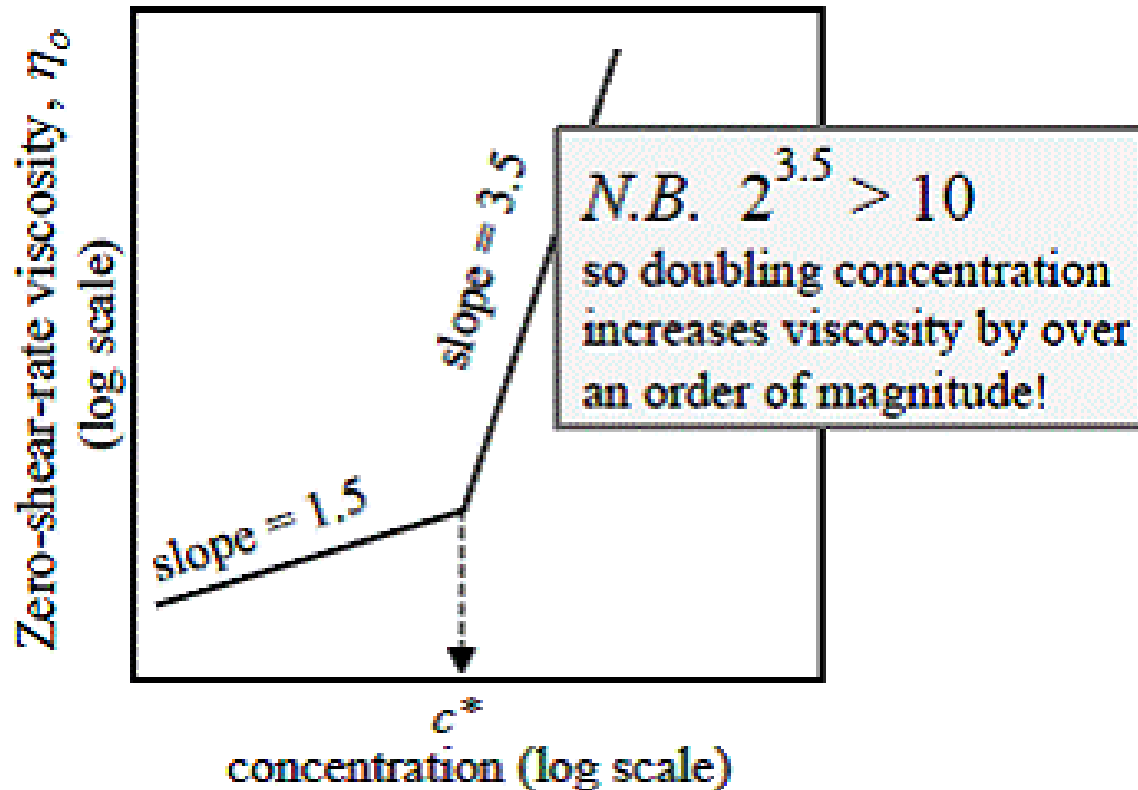


Figure 2.6 The zero-shear-rate viscosity of a polymer solution versus polymer concentration, showing the critical overlap concentration c^* [from 4]

At high concentrations, there is the appearance of another interaction which is called entanglement where the chains are completely intertwined and entangled and continuously slide over each other as they move in the solution. This second critical concentration is denoted by c^{**} and again the behaviour is also different. The various regimes of polymer solution are; dilute for $c < c^*$, semidilute ($c^* < c < c^{**}$) and concentrated when $c > c^{**}$.

The elasticity in concentrated solutions is due to the persistence of tension between the entanglements as the entangled chains slide over each other. This elastic behavior is present at very short time when the entanglements are still present but reverted to the viscous behavior when it has lost the entanglements and the chains are fully stretched.

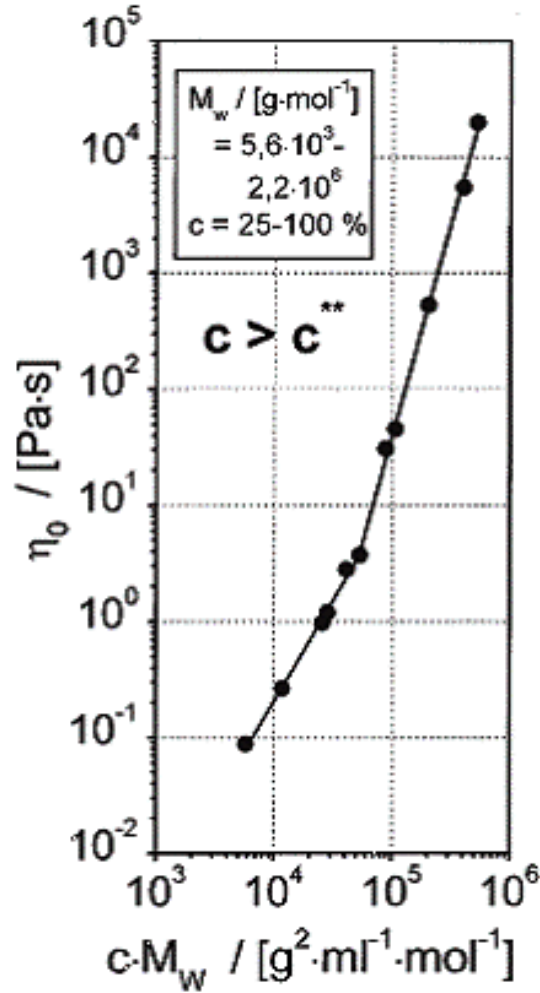


Figure 2.7 Zero-shear viscosity (η_0), as a function of the $c \cdot M_w$ (molecular weight and concentration) for narrowly distributed polystyrenes in toluene, $T=58^\circ\text{C}$: The concentration lies above the critical concentration, c^{**} .

This change in gradient is also evident in a plot of zero shear viscosity- $c[\eta]$; the overlap parameter.

Above the critical concentration the increase in the zero-shear viscosity with cM_w is proportional to $M_w^{3.4}$, figure 2.7 [3]

Experimentally, the intrinsic viscosity can be determined by measuring the viscosity of a polymer solution in varying concentration and using either the Huggins or Kraemer Equations (5) and (6) respectively.

$$\frac{\eta_{sp}}{c} = [\eta] + K_H[\eta]^2 c \quad (5)$$

$$\frac{\ln \eta_{rel}}{c} = [\eta] - K_k [\eta]^2 c \quad (6)$$

The intercept of the linear regression to the equation is the intrinsic viscosity and the slope used to calculate the Huggins and Kraemer constants. Clasen and Kuclike (2001) [3] used the plot of η_{spec} as a function of the overlap parameter to generate equation to predict the structure-property relationship of cellulose derivatives. The structure-property relationship is the line in figure 2.8 according to the equation $\eta_0 = 0.891 + 0.891 c[\eta] + 6.11 * 10^{-1}(c[\eta])^2 + 1.28 * 10^{-1}(c[\eta])^{4.24}$

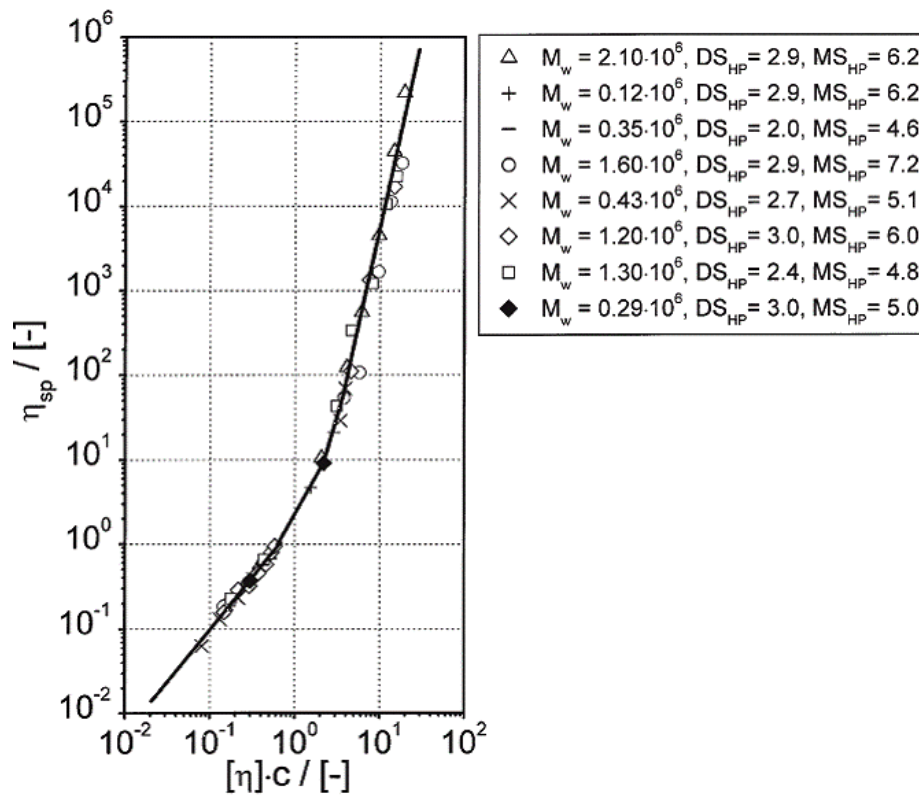


Figure 2.8 The specific viscosity (η_{sp}) as a function of the overlap parameter, $c[\eta]$; for hydroxypropyl cellulose (HPC) in aqueous solution (M_w (g/mol)). The continuous line represents the structure-property relationship. [3]

Many authors have tried to derive other expression for calculating the intrinsic viscosity. Among these expressions is the Martin's equation (7) which according to Abdel-Azim et al (1998) [24] is the least

concentration dependent. A linear fit to a plot of $\log \frac{\eta_{sp}}{c^2}$ vs. c gives the intrinsic viscosity and the Martin's constant K_M

$$\log \frac{\eta_{sp}}{c^2} = \log[\eta]_M + K_M[\eta]_M c \quad (7)$$

2.2 Molecular weight Determination

As stated above molecular weight and molecular weight distribution greatly influence the solution properties of polymer solution. The formation of entanglements of polymer coils above a critical molar mass leads to strong changes in the viscoelastic behaviour. Very different molar mass distribution of cellulose has been found for the same polysaccharide according to the source of plant, location and climatic conditions [8]. The precise value of molar mass is difficult to get and so average values are gotten from experiments. The molar mass averages used can be calculated from equation 8 [3] below and for $\beta = 0$, we have number average M_n , $\beta = 1$ - weight-average M_w , and $\beta = 2$, centrifuge-average M_z . The viscosity average M_η is calculated by equation 9[3] and lies between M_w and M_n .

$$M_x = \frac{\sum_i n_i M_i^{\beta+1}}{\sum_i n_i M_i^\beta} \quad (8)$$

$$M_\eta = \left(\frac{\sum_i n_i M_i^{1+a}}{\sum_i n_i M_i} \right)^{1/a} \quad (9)$$

In the above equations n_i is the number of moles of polymer species with molar mass M_i and a is the exponent of the Mark-Houwink-Sakurada relationship which depends on the polymer/solvent pair used in the viscosity experiment. Also, the polydispersity index (PDI) is stated which is the ratio of M_n and M_w and the degree of polymerization (P) is calculated from the weight average molar mass.

For more precise value for engineering applications, various methods have been developed for finding the molecular weight and molecular weight distribution. Membrane osmometry (by means of ultracentrifugation and light scattering) does not require knowledge of the chemical and physical structure but molar mass can be calculated

2.3 Capillary Breakup Extensional Rheometer (CaBER)

Capillary Breakup Extensional Rheometry is a technique suitable for the determination of the extensional rheological properties of a fluid. The technique employs the action of surface tension and capillary forces on a fluid bridge formed by applying a step strain to it. The step strain and the capillary forces cause the bridge to be unstable and begin to collapse. The liquid bridge thins and finally breaks into two. The breakup or thinning of the liquid bridge is governed by the capillary forces, surface tension and internal rheological forces arisen from deformation and therefore rheological properties can be studied by observing the thinning or breakup of this liquid bridge. For Newtonian fluids the thinning is said to be linear with time and exponential for viscoelastic fluids [18].

The CaBER rheometer is made of two plates between which the fluid to be tested is placed. The upper plate is moved imposing a step strain to the fluid column and after it stops, the decrease in the fluid midpoint diameter is measured with time with the help of a laser micrometer. The fluid configuration before and after the stretching can be seen in figure 2.9.

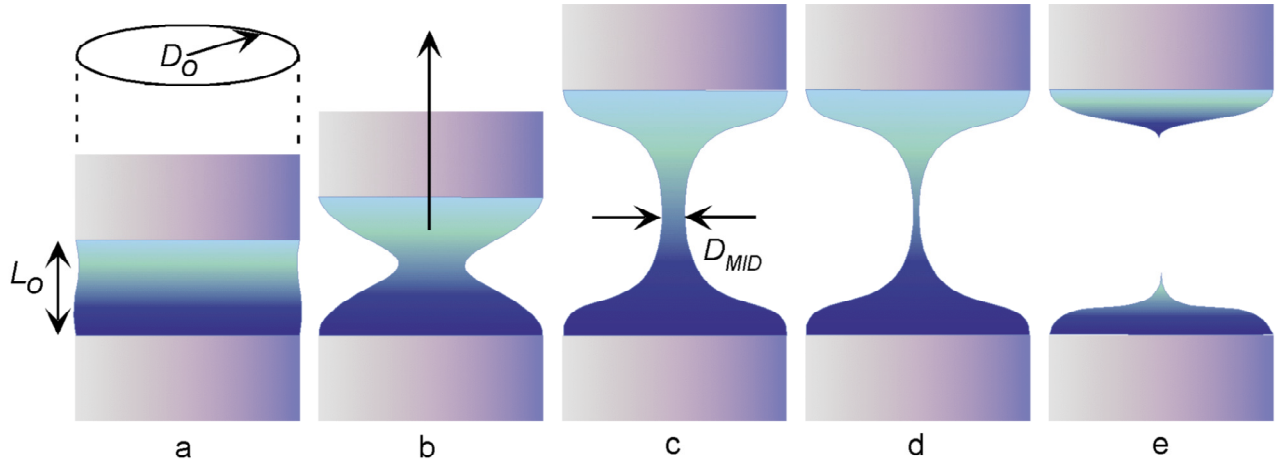


Figure 2.9 Fluid configurations before stretching (a), during stretching (b), immediately after stretching has stopped (c), during capillary drainage (d) and after breakup (e). L_0 is initial length, D_0 is diameter of plates.

The plate are displaced according to an exponential equal to $L = L_0 \exp(\dot{\epsilon}t)$, $\dot{\epsilon}$ is the strain rate and t is time. The strain rate on the fluid column at the midpoint can be given by equation 10. Integrating equation 10 gives the strain in the fluid column with time, which is the Hencky strain at the axial mid plane (equation 11).

$$\dot{\epsilon} = -\frac{2}{R_{mid}} \frac{dR_{mid}}{dt} = \frac{dL}{L} \tag{10}$$

$$\epsilon(t) = 2 \ln \left[\frac{R_0}{R_{mid}(t)} \right] \tag{11}$$

After the end of step deformation, the decrease in the midpoint diameter is governed by the action of surface tension and the viscosity or viscoelasticity. It has been stated that during the necking and breakup of the fluid filament, the elastic tensile stresses resist the pinching caused by capillary action, as a result the tensile stresses in the polymeric fluid grow and the polymer chains tend to elongate at the local region near the breakup.[1]

The step strain must be faster than the viscoelastic relaxation time in the fluid (equation 12) and the capillary time to breakup (equation 13) [1]. In analysing the filament thinning and breakup, one of the assumptions used is the axial symmetry about the midplane which is affected by gravitational force. The gravitational force affects the symmetry and leads to a weak axial flow so that the filament sags and there is more fluid below the midplane. The extent of the effect can be accounted for by using the Bond number, B_0 (equation 14) which represents the sagging effect compared to the opposing capillary forces. For $B_0 \ll 1$ (i.e very low Bond number) gravity can be neglected but becomes important with increasing Bond number [17]

$$\dot{\epsilon} \gg 1/\lambda_1 \quad (12)$$

$$\dot{E} \gg 2\sigma/\eta_0 D_0 \quad (13)$$

$$B_0 = \frac{\rho g D_0^2}{4\sigma} \quad (14)$$

Here; λ_1 is the relaxation time, D_0 the initial diameter of the fluid, ρ density of the fluid, g acceleration due to gravity, η_0 zero shear viscosity and σ surface tension. The force balance on a fluid column is given by equation (15) which for a particular fluid model the equation can be solved stating assumption that are applicable to that model. In the proceeding section the analysis for a Newtonian fluid is performed to derived an equation governing the rate of decrease of the liquid bridge diameter or radius starting with equation 15.

$$\frac{F_z(t)}{\pi R(z,t)^2} = 3\eta_s \left(-\frac{2}{R} \frac{\partial R}{\partial t} \right) + [\tau_{zz} - \tau_{rr}] + \frac{\sigma}{R} \{1 + \phi(R', R'')\} - \frac{\rho g R_0^2 Z_0}{R^2} \quad (15)$$

*Tensile Force
In column*

*Viscous
Stress*

*Non – Newtonian
Stress*

*Capillary
Pressure*

*Gravitational
Body Force*

2.3.1 Extraction of Viscosity for a Newtonian Fluid

The Assumptions that can be made for a Newtonian fluid in 1D are;

- Self similar
- No gravitational contribution
- The tensile force at the midpoint as the radius turns to zero
- The axial curvature radius can also be neglected

The force balance in equation 14 reduces to;

$$3\eta_s \left(-\frac{2}{R_{mid}} \frac{dR_{mid}}{dt} \right) = \frac{2\pi\sigma R_{mid}}{\pi R_{mid}^2} - \frac{\sigma}{R_{mid}} \quad (16)$$

After cancelling and rearranging equation 16, we have; $dR_{mid} = -\frac{\sigma}{6\eta_s} dt$ (16b)

Integrating gives $R_{mid} = -\frac{\sigma}{6\eta_s} t + K$ (17)

Using the initial boundary conditions; at $t = 0$, $R_{mid}(t) = R_1$ – radius of the midpoint when the plate has stopped moving, equation 17 becomes;

$$R_{mid}(t = 0) = 0 + K = R_1$$

$$K = R_1$$

$$R_{mid}(t) = R_1 - \frac{\sigma}{6\eta_s} t \quad (18)$$

In extracting the viscosity of the Newtonian fluid from such an experiment as the CaBER, a linear regression can be done on the later part of the curve in the diameter against time plot. The later part of the curve can be used because as time passes the capillary forces dominates any gravitational forces which affects the rate of decrease of the diameter at the initial and intermediate times [2]

The slope can be equated to $-\frac{\sigma}{6\eta_s}$ and knowing the surface tension from other experiments the viscosity can be calculated.

Equation 18 can be written in a different form if we are consider that the midpoint diameter breaks at a critical time t_c , so $R_{mid}(t_c) = 0$. Therefore, $R_1 = \frac{\sigma}{6\eta_s} t_c$ and substituting this into equation 18 gives equation 18b. Also the ratio $\frac{\sigma}{\eta_s}$ is called the capillary velocity related to the characteristic rate of

$$R_{mid}(t) = \frac{\sigma}{6\eta_s} (t_c - t) \quad (18b)$$

necking in the Newtonian fluid thread. This velocity extracted from a fitting to data from experiment varies from mathematically calculating it using values of the parameters from other experiments. This difference has been found to be due to axial inhomogeneity in the liquid bridge.[2] Numerical simulation and experiment has suggested a modification to equation 18 to equation 19 to take into account these variations, where X is a dimensionless variable. Values of X as given by many authors with different similarity solutions can be seen in table 2.1. [2]. McKinley and Tripathi (2000) determined that the best X value for a Newtonian fluid (viscous) is the Papageorgiou factor (0.7127)

$$R_{mid}(t) = R_1 - \frac{(2X-1)}{6} \frac{\sigma}{\eta_s} t \quad (19)$$

		X	$(2X - 1)/6$	Notes
Local Force balance	Re = 0	1	1/6	Axially uniform thread
Rennardy (1995)	Re = 0	-	-	Three different similarity regimes
Papageorgiou (1995)	Re = 0	0.7127	0.0709	Valid for viscous fluid filament
Eggers (1993, 1997)	Re > 0	0.5912	0.0304	Universal similarity solution
Brenner et al. (1996)	Re > 0	0.5912	0.0304	Countably infinite similarity
		0.5324	0.0108	solution

Table 2.1. Summary of the different similarity solutions obtained for the breakup of slender columns of a viscous Newtonian fluid [2].

The force balance has been solved for different kinds of fluids and the solution for the decrease in the midpoint diameter is presented in table 2.2. For a particular fluid model the diameter versus time can be gotten from the experiment and appropriate regression done to determine the parameters

Constitutive Model	Form of Solution	Parameters found from regression to data
Newtonian, $\tau = \eta_s \dot{\gamma}$	$D_{mid}(t) = 0.142(\sigma/\eta_s)(t_c - t)$	$t_c, \sigma/\eta_s$
Power-Law Fluid $\tau = K\dot{\gamma}^n$	$D_{mid}(t) = 2^{1-n} (0.142)(\sigma/K)(t_c - t)^n$	$t_c, \sigma/K, n$
Upper Convected Maxwell	$D_{mid}(t) = D_0 (GD_0/\sigma)^{1/3} \exp(-t/3\lambda_c)$	$\lambda_c, G/\sigma$

Table 2.2 Solution to force balance for different kinds of fluids

2.3.2 Apparent Extensional Viscosity

The extensional viscosity of Newtonian fluids can be calculated from equation 18 but this analysis is not valid in the case of non-Newtonian fluids. However it is not easy to determine prior what kind of behaviour or expected, therefore some other method must be used for the data analysis. The extensional

viscosity is found in the evolution of the midpoint diameter in a filament breaking experiment and the thinning process is governed by rheology and the effect of surface tension of the fluid. An apparent extensional viscosity can therefore be related to the evolution of the midpoint diameter as its first derivative with time (equation 20) thus assuming the Newtonian solution still holds.

$$\overline{\eta}_{app} = \frac{-\sigma}{dD_{mid}/dt} \quad (20)$$

However it is difficult to determine directly the true derivative of the experiment data as diameter readings are quite noisy. Therefore to find the derivative, the midpoint diameter change with time can be resolved with a function, generally valid for any type of fluid and which agrees with the observation of an exponential decrease of diameter with short and intermediate time followed by a linear behavior at late times.

For polymeric solutions the former behaviour can be associated to chains become fully stretched and the elastic stresses cannot longer grow to resist the increasing capillary pressure. The polymer behaves as a viscous anisotropic Newtonian fluid with a viscosity equal to the steady-state extensional viscosity.

[1] The global function is given in equation 21 [1]

$$\frac{D_{mid}(t)}{D_1} = ae^{-bt} - ct + d \quad (21)$$

Where a , b , c and d are fitting parameters, b^{-1} is related to the largest relaxation time of the fluid and c^{-1} the steady-state extensional viscosity. A fitting of the data to this function can be done and the parameters used to find the derivative of the curve and the apparent extensional viscosity calculated. At long times when the polymer chains are fully stretched and the decrease in the midpoint diameter is linear, a steady-state apparent extensional viscosity can be determined which shows a constant value.

The asymptotic value of equation 21 can be found and used to calculate the steady-state extensional viscosity.

Sometimes the apparent extensional viscosity is expressed in terms of a dimensionless quantity known as the Trouton ratio. The Trouton ratio is expressed as the ratio of the transient extensional viscosity to the zero-shear viscosity in the fluid (η_0) equation (22). For a Newtonian fluid the Trouton ratio is 3 according to equation 1. Figure 2.10 shows a graph of apparent viscosity as a function of strain for three fluids where for a Newtonian fluid shows a horizontal line.

$$Tr \equiv \frac{\overline{\eta_{app}}}{\eta_0} \tag{22}$$

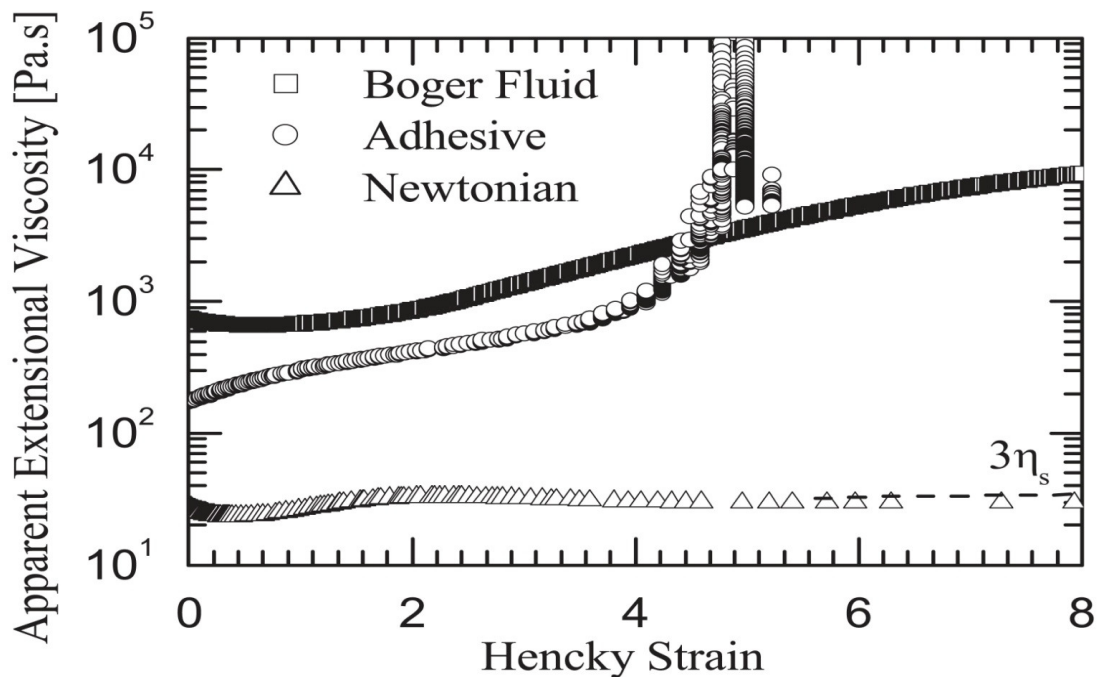


Figure 2.10 Apparent Extensional viscosity as a function of Hencky strain for three different fluids [16]

2.4 Cellulose Acetate

Cellulose acetate is a synthetic polymer derived from acetylation of plant substance cellulose. Cellulose is a natural polymer obtained from wood fibers. It is made up of the repeating unit of glucose: with formula $C_6H_7O_2(OH)_3$ and structure in figure 2.11

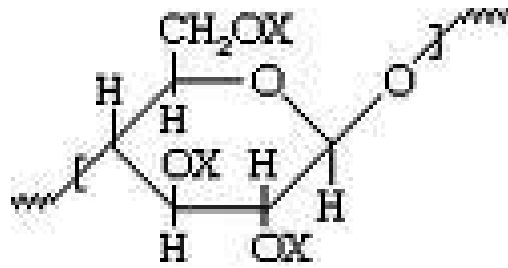


Figure 2.11 Chemical structure of cellulose acetate with X representing the acetyl group (CH_3-CO). In unaltered cellulose X is H (hydrogen) meaning the presence of three(3) $-OH$ (hydroxyl groups). The $-OH$ groups forms strong hydrogen bonds among cellulose molecules which cannot be decomposed by heat or solvents without chemical decomposition of the whole molecule. Acetylation is used to make cellulose more processable during heating or dissolution by a replacement of the hydrogen (H) in the hydroxyl group with acetyl group (CH_3-CO). The resulting cellulose acetate can be dissolved in solvent or softened by heat into melt which can be spun, cast or molded.

Cellulose acetate is produced by treating cellulose with acetic acid and acetic anhydride in the presence of sulphuric acid (H_2SO_4) as catalyst. The resulting material is called primary cellulose acetate or cellulose triacetate which is soluble in chloroform but not in most solvents, so it is sometimes called chloroform soluble acetate. When the triacetate is dissolved in water there is partial reverse of the acetylation to form the less substituted cellulose diacetate which is soluble in cheap solvent like acetone and is known as acetone soluble acetate. The advantage of cellulose acetate lies in the low toxicity and low or almost non-flammability. Also it is produced from renewable sources and is biodegradable at least after pretreatment.

2.4.1 Uses of cellulose acetate

In the textile industry, cellulose acetate is spun into silk yarns mostly used in women apparel. Moreover, it is used as filter tow in making cigarette filters because of its unique retention behaviour. Cellulose triacetate and diacetate in combination with plasticisers as well as mixed esters can be used to produce transparent thermoplastics with excellent clarity and mechanical properties. They have good resistant to embrittlement and good electrical insulation. Plasticised or ester mixed cellulose acetate can be injection moulded or extruded to produce tool handles, toothbrush handles, combs, barrettes (hair pin/clip for women) and toys. In the automobile industry they can use in the making of parts like steering wheels, and signal glasses. An important application is in the production of frames for spectacles

Cellulose acetate films are used mainly in the film industry as photographic films and also for professional motion picture films. They are also used in the construction of security glass for automobiles and electrical insulation films for condensators. There is the growing demand for the use of cellulose acetate films in modern LCD (Liquid crystal Display) flat screens.

2.4.2 Solubility of cellulose Acetate

Solubility is the ability of a solute (polymer molecule) to dissolve in a solvent to form a homogenous solution. Because of the wide difference between polymer molecules and solvent, it is difficult to dissolve polymer in a many solvent. Some polymers dissolve easily in a particular solvent while others require heating or stirring to have a good dissolution while cross-linked polymers are taught not to dissolve but rather swell. Swelling is the increase in the hydrodynamic radius of a polymer molecule segment forming a sphere due to strong interaction between solvent and polymer against that of the polymer – polymer interaction. The solubility of a polymer molecule may depend on the following; molecular weight, degree of crystallinity, extent of branching and temperature.

$$\delta = \left(\frac{\Delta E}{V}\right)^{1/2} \quad (23)$$

$$\delta^2 = \delta_d^2 + \delta_p^2 + \delta_h^2 \quad (24)$$

The solubility parameter (δ) is the measure of how a material will dissolve in another to form a solution. Solubility parameter is defined as the square root of the cohesive energy, where the cohesive energy is the evaporation energy (ΔE) divided by the molar volume (V), which can be mathematically represented as in equation (23). As a general rule, materials with very similar solubility will be miscible to form good solutions. Hansen proposes a solubility parameter that is made up of three contributing factors; dispersive (d), hydrogen bonding (h) and polar (p) contributions and therefore modified the solubility parameter to be as equation (24)

The solubility of cellulose acetate also depends on the degree of substitution (DS), for example cellulose acetate with DS of 2 – 2.5 has been found to dissolve in solvents like acetone, dioxane and methyl acetate while those with higher DS or higher acetylation are soluble in dichloromethane [12]. In general it was found that acetic acid is a good solvent for cellulose acetate with DS greater than 0.8.[12]. In the experimental results of Fisher et al (2008) [12] on the solubility of different kinds of cellulose acetate in different solvents, they found out that all cellulose acetate used were soluble in acetone and dichloromethane – methanol mixture (80:20). However, the cellulose acetate solutions showed different turbidity. Turbidity is the decrease in the transparency of a liquid due to the presence of undissolved substances.

2.4.3 Structure of cellulose derivatives in solution

The study of the properties of cellulose derivatives solution can be done with the help of tools that rely on molecular mass and geometric shape determination available by static and dynamic light scattering. These studies according to Rustemeyer (2004) [9] show that there are two structural forms in dilute solutions. One is the presence of molecularly dispersed solutions in which the macromolecules are separated from each other and surrounded by solvents molecules. This can be obtained when the cellulose molecules are fully substituted and strong polar interactions are excluded between macromolecules and solvents, or when the strong polar bonds are shielded or not effective; Figure 2.12(a). The second type is when there is strong hydrogen bonds interaction or incompatible interactions in solution such that irreversible aggregation occurs and the molecules cannot be separated. Moreover, one can expect that the interactions are not strong and reversible associations or clusters may be formed. Figure 2.12(b)

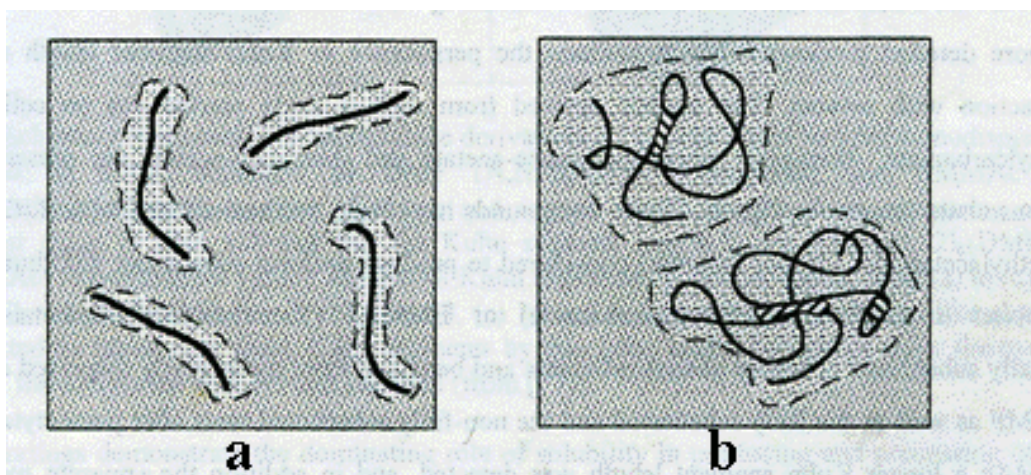


Figure 2.12 schematic representations of single semi-flexible macromolecules in a molecularly dispersed solution. **a** - for low molecular mass and **b** - high molecular mass. The dashed line indicates solvent shell. [9]

2.4.4 Structural characterization of cellulose acetate

The properties of the acetate may also depend on the average distribution of the acetyl groups at the three possible sites of the anhydroglucopyranose unit and the distribution along the chain. These affect the crystallinity index leading to various changes in properties when in solution.

Solid state characterization can be done by spectroscopy (IR and NMR), diffraction (X-ray or electron scattering). Also the crystallite size, disorder and motion of the atoms may be of interest in the determination of the mechanical properties. For crystal polymers two kinds of X-ray diffractograms are available; Debye-Scherrer pattern from samples with isotropic distributed crystallites figure 2.13 (b) and Fiber patterns where the crystallites are uniaxially oriented in native fibers in stretched or drawn sample figure 2.13 (a). [9]

There have been two kinds of crystal structure for cellulose triacetate which produces different Debye-Scherrer diffractograms. There are called CTA I from heterogeneous acetylated native cellulose I and CTA II from reacting regenerated cellulose II as starting material. CTA II can also be achieved by superheated steam treatment with any dissolving process. CTA II cannot be converted to CTA I

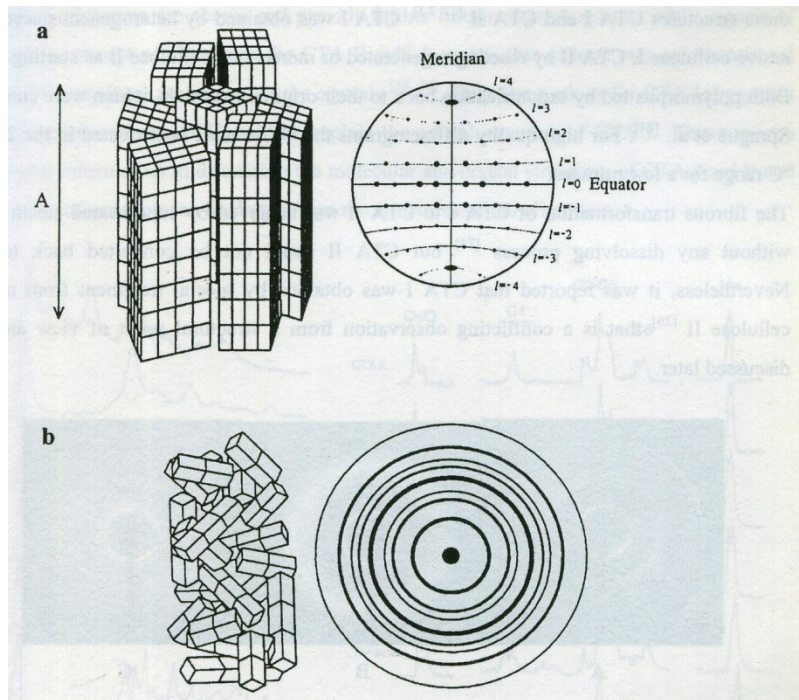


Figure 2.13 representation of distribution of crystallites and the resulting diagrams (a) uniaxially distributed crystallites around A leading to a fiber pattern, (b) Isotropically arranged crystallites producing a Debye-scherrer pattern of concentric rings[9]

2.4. 5 Rheology of Cellulose Acetate Solution

Knowledge of the rheological properties of cellulose acetate solution is very important in industrial application since for example knowledge of the intrinsic viscosity gives a measure of the degree of polymerization or the molecular weight. [13] The conformation of polymer in solution can depend on the following factors; chemical structure of the polymer, molar mass, temperature and solvent. [3] Also the concentration of solutions determines the flow properties during processing in industry. The effect of shear rate on the shear viscosity of a cellulose acetate solution prepared in a solvent mixture of 42.3% acetone and 29.2% formamide is shown in figure 2.14 the rheological characterization was done with a rotational rheometer. [14].

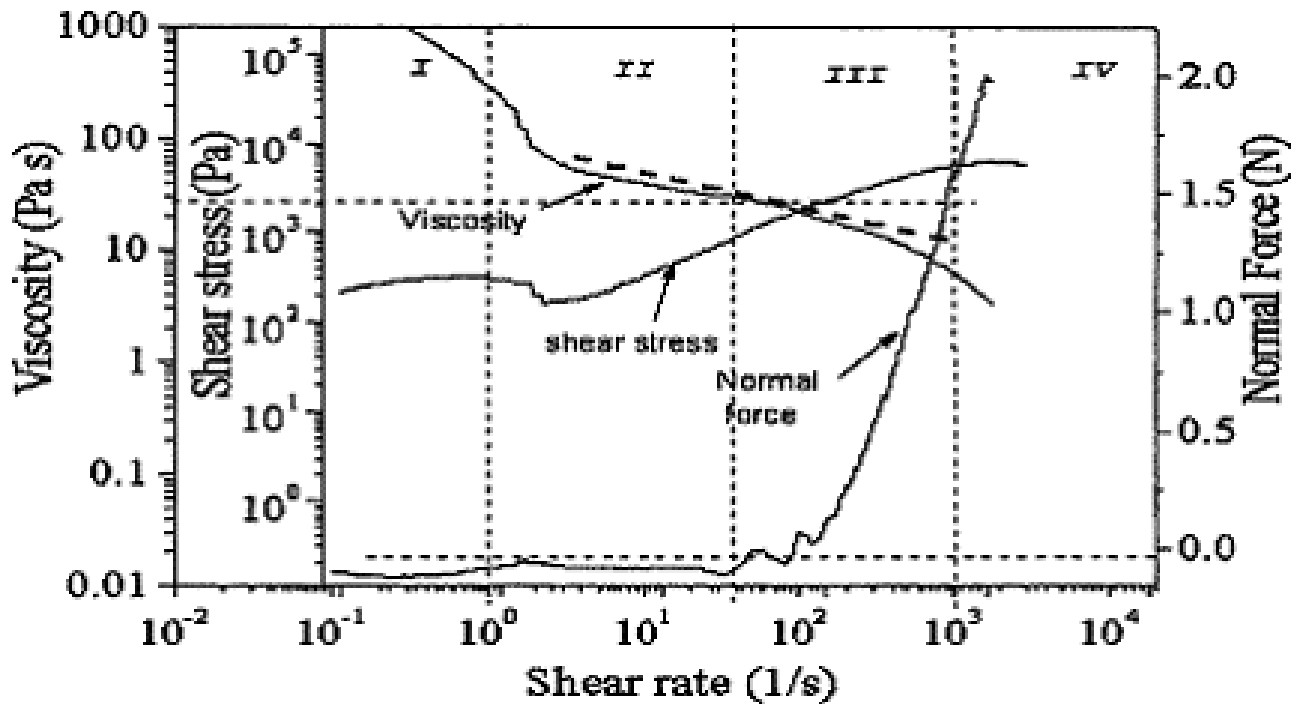


Figure 2.14 Flow curve with normal force at 25 °C for 27% CA, 43.8% acetone and 29.2% formamide. (Ratio of acetone to formamide=1.5). [14]

The figure shows four different regions (I–IV). The first region according to the authors shows dispersion in data as a result of equipment limitation. In region II the dope (polymer solution to be electrospun) behaves like a Newtonian fluid, where the viscosity of the dope solution is almost constant. As the shear rates increases (region III), the cellulose dope solution displays classical shear thinning power law properties given by $\eta = k\dot{\gamma}^{n-1}$ where k is a measure of the consistency of the fluid, $\dot{\gamma}$ is the shear rate and n is a degree of non-Newtonian behavior. The power law relates to the thickness of the dope where the higher the k value, the higher is the apparent viscosity, whereas the power law index relates to the shear thinning behavior. The lower the n value the greater the shear thinning and molecular alignment.

As the shear rate increases, there is a point where the gradient of the viscosity decrease changes called; the second critical shear rate (SCSR). The rapid decrease in viscosity with increase in shear rate was

explained to be due to high rotational speed resulting in sample loss through centrifugal force in rotational rheometers (region IV). [14]

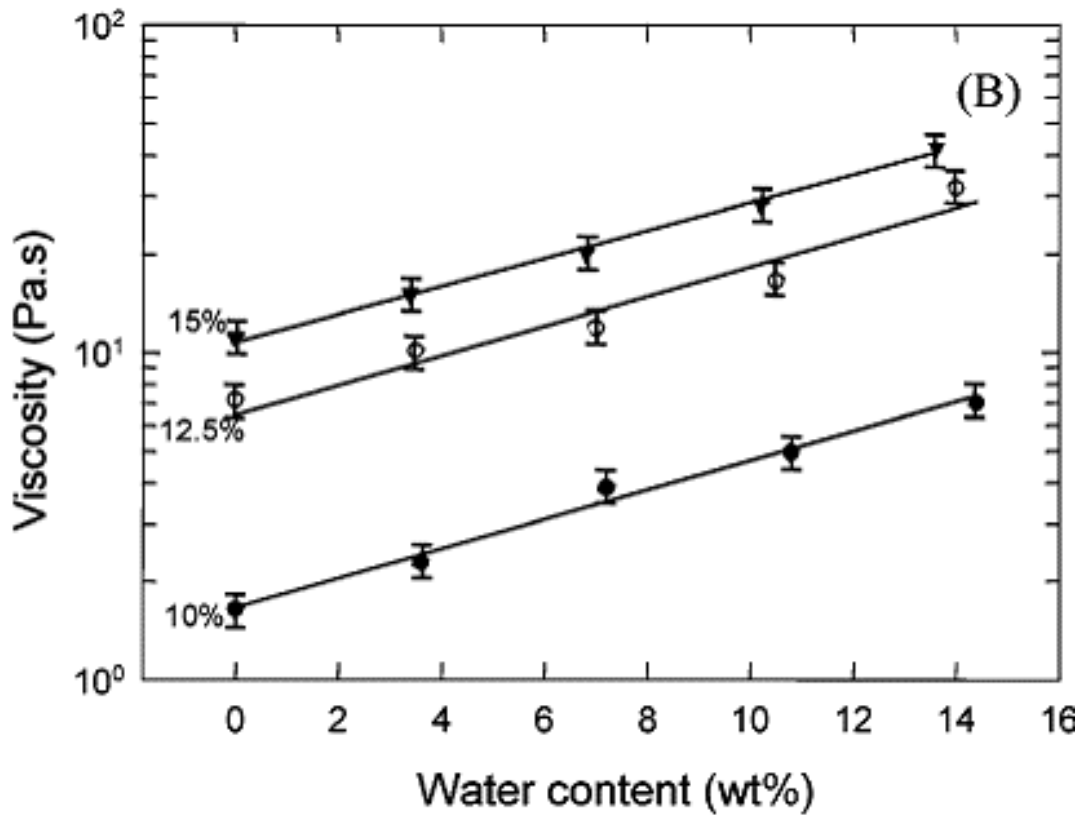


Figure 2.15 viscosity as a function of water content obtained at shear rate of 1 s^{-1} for CA concentrations of 10 (●), 12.5 (○), and 15 (▼) wt %. [15]

Figure 2.15 shows a graph of shear viscosity versus water content for different concentration of cellulose acetate in solution of N,N-Dimethylacetamide (DMA). The graph shows the low shear viscosity (shear rate 1 s^{-1}) to increase by almost an order of magnitude when the cellulose acetate concentration is increased from 10 to 15 wt %. Also, the low-shear viscosity increases exponentially with increased water content, with the exponent being same for all three cellulose acetate concentrations studied. The addition of water leads to an opaque self-supporting gel-like material [15]. It can also be seen that the viscosity increases with increasing concentration of cellulose acetate.

The storage modulus (G') also shows a shift to higher values with increase in cellulose acetate concentration and water content. The elastic modulus shows a power law behavior with water content;

the power law exponent varies between 10.9 – 12.5 for concentration from 15, 12.5 and 10% wt cellulose acetate according to [15]. (Figure 2.16)

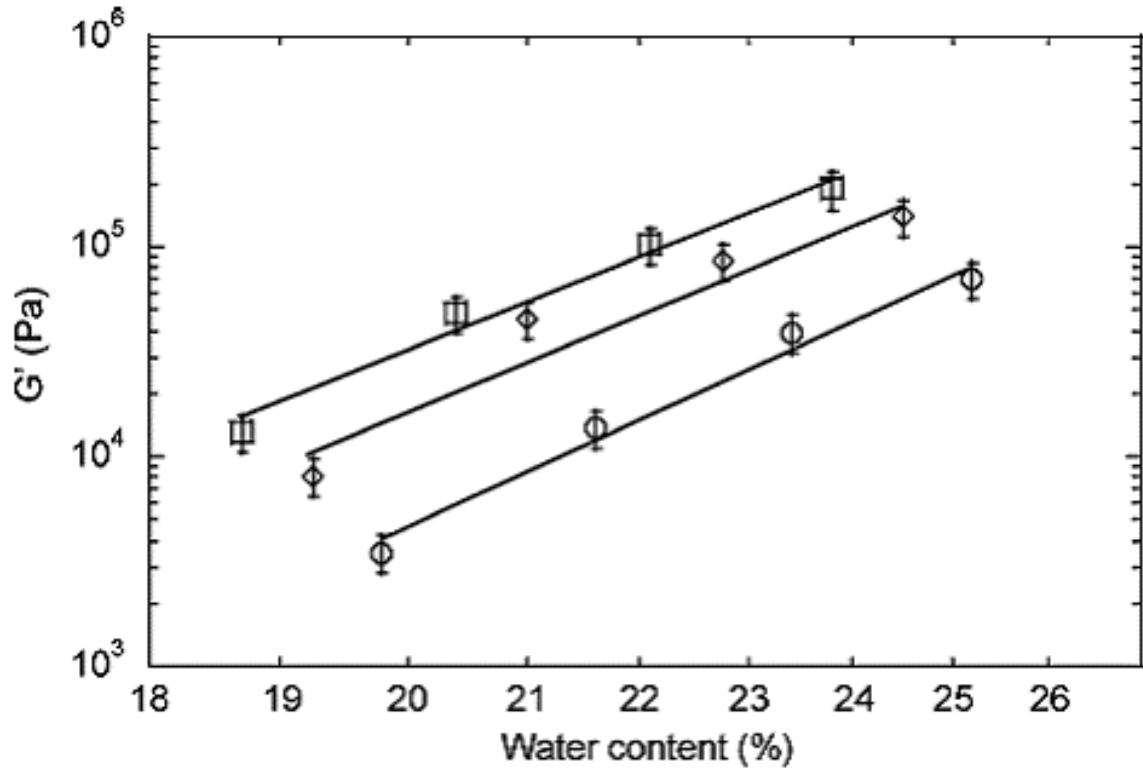


Figure 2.16 Effect of CA concentration and water content on elastic (G') moduli. Cellulose Acetate concentrations: \square 15, \diamond 12.5, and \circ 10 wt % (1 rad s^{-1}).

2.4.5 Thermal properties

Important processing quantities for crystalline polymers are the melting temperature and the glass transition temperatures. The melting temperature can easily be determined by DSC (Differential Scanning Calorimetry) or DTA (Differential Thermal Analysis) because it is a first order equilibrium which involves enthalpy change. Glass transition temperature on the other hand is a non-equilibrium transition involving the onset of segmental chain motion and can be determined by DSC or DMTA (Dynamic Mechanical Thermal Analysis). In DSC T_g (glass transition temperature) is recorded as a change of the specific heat and in DMTA as a drop in storage modulus or a peak in loss modulus.

Static measurements are DSC, DTA and TGA (Thermal Gravimetric Analysis). DTA measurement showed $T_m = 290^\circ\text{C}$ [9] and three transition temperatures between 186°C to 213°C [9]. The decomposition temperature $T_d = 356^\circ\text{C}$ [9] by TGA and the narrow interval between T_m and T_d makes processing from the melt difficult. There is small dependence of molecular weight on T_g showing an increase in T_g from low molecular weight to high molecular weight. There is a marked dependence of T_g , T_m and T_d on the degree of substitution (DS) as can be seen in figure 2.17 and equation 25 for T_g [9]. It can be seen from also figure 2.15 that the glass transition temperature decreases with increasing the degree of substitution of the acetate. The decomposition temperature shows an initial decrease followed by an increase with DS, while the lowest melting temperature is around DS = 2.5.

$$T_g(K) = 523 - 20.3 DS \quad (25)$$

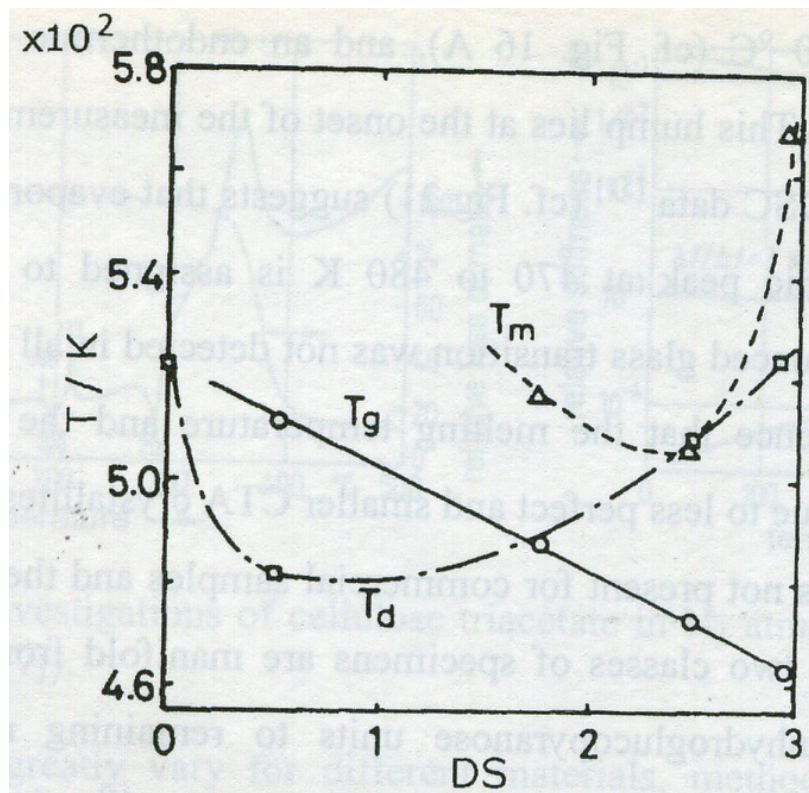


Figure 2.17 The dependence of glass transition temperature T_g , melting temperature T_m and decomposition temperature T_d on the average degree of substitution DS. [9]

Dynamic measurement gives the dependence of the dynamic modulus on temperature or frequency. DMTA analysis of cellulose acetate shows a decrease in T_g with DS in agreement with equation 25 and a lowering of the peak height with increasing crystallinity.

2.5 Electro Spinning

Electro-spinning is a process of producing fibers from solutions and melts with diameters ranging from few micros to nanometers. Electro-spun fibers can be used in nanocomposites, biomedical engineering, protective clothing, and sensors [7]. Electro-spinning employs the competition between the surface tension of the fluid and an electrostatic force applied to the fluid to form fibers whose diameter and morphology depends on the elasticity of the solution. During the electro-spinning process, if it is driven by the surface tension, Rayleigh instability develops, which tends to break the jet into droplets and becomes more important as the diameter of the jet becomes smaller [19].

External electric field, surface charges and solution elasticity tend to suppress the Rayleigh instability and stabilize the jet. As a result, the surface tension, the charge density and the solution elasticity are thought to play large roles in determining the electrospinnability of polymer solutions. The charged liquid is separated some distance from a second electrode (target) of opposite polarity to establish a static electric field. A so-called Taylor Cone forms due to the competing forces of the static electric field and the liquid's surface tension. For liquids with a finite conductivity, charged droplets are dispersed from the tip of the Taylor Cone and are delivered to the target. If the liquid consists of a polymer melt or a polymer in solution and the concentration of that polymer is sufficiently high to cause molecular chain entanglement, a fiber, rather than a droplet, is drawn from the tip of the Taylor cone.

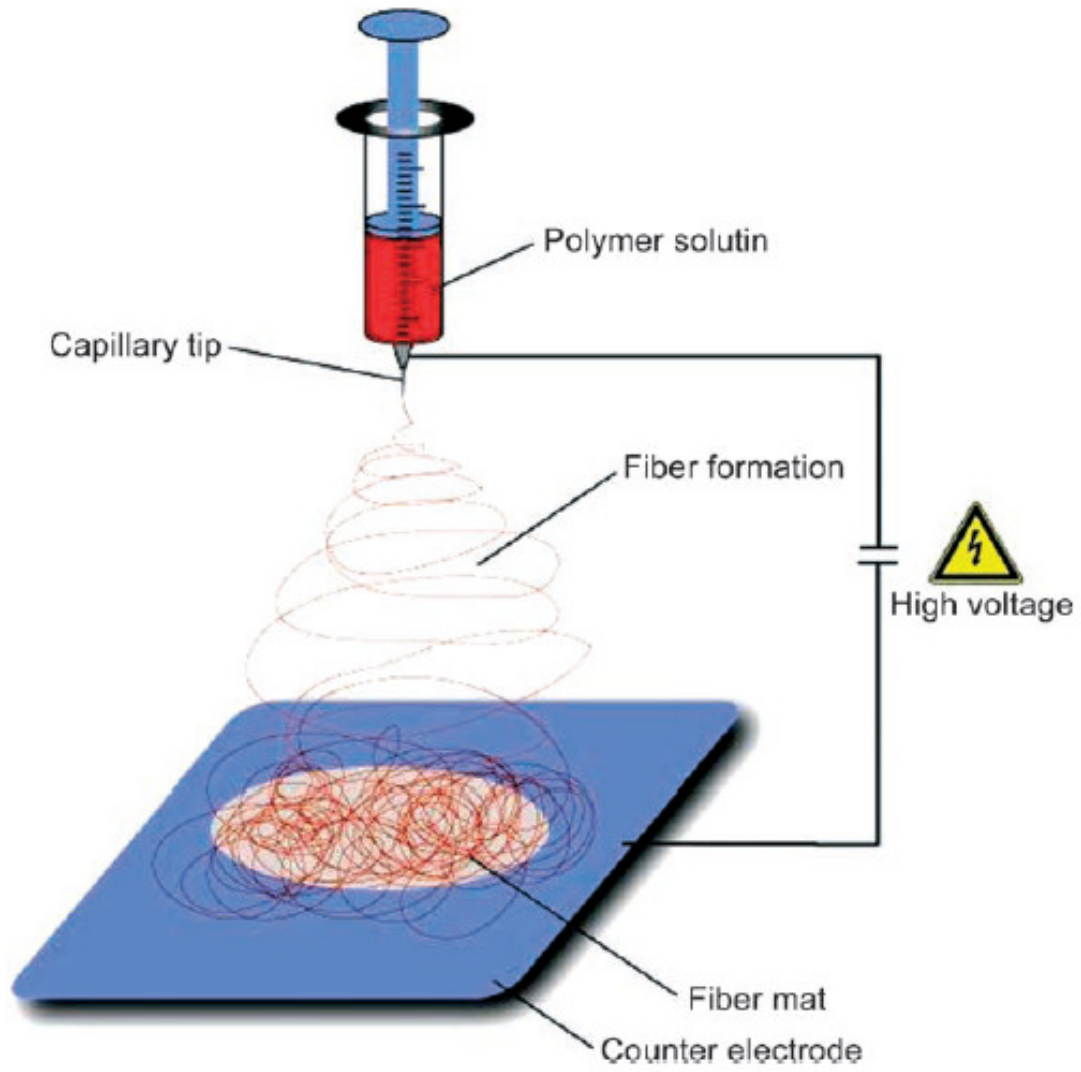


Figure 2.18 Laboratory setup for an electrospinning experiment with a perpendicular arrangement of the electrodes [8]

3.0 Methodology

This chapter contains the details of the experimental work done in this project. Three types of cellulose acetate from three different manufacturers namely; Società acetate, Celanese UK and Celanese USA are used in this project. The solvent for the solution is a mixed solvent of dichloromethane (CH_2Cl_2) and methanol (CH_3OH) in a ratio of 75:25 (3:1). Solutions of concentrations 7, 10 and 12.5 % wt/v of each sample are prepared and capillary break up test were performed using CaBER I (Cambridge Polymer Group) at temperatures 5, 10, 15 and 20 °C. The data from the CaBER I is analysed to extract useful material properties like apparent extensional viscosity.

3.1 Material Choice and Sample preparation

Various concentrations of cellulose acetate solution were prepared using as solvent a mixture of dichloromethane and methanol (75:25). The choice of this solvent mixture stem from the fact that it is a good solvent for cellulose acetate with degree of substitution greater than 0.8 according to Fischer et al (2008) [12]. Of course this solvent mixture is not the only suitable solvent for cellulose acetate, for example in the thesis of Davide Colombo [24], ethylacetate was shown to be a valid solvent but was not suitable for electrospinning. The selected solvent mixture resulted electrospinnable in tests performed in University of Bologna.

The cellulose acetates are dried in an oven at 70°C for four (4) hours after which they are placed in desiccators to prevent moisture from coming into contact with the material. The material data for all three are shown in table 3.1 as determined from Gel Permeation Chromatography (GPC) [23]. For example for a 50ml solution of 10% wt/v concentration, we have to measure 37.5ml of CH_2Cl_2 and 12.5ml of CH_3OH with 5g of cellulose acetate. The solutions were prepared by stirring it between 4 to 6 hours using a magnetic stirrer and stored in a refrigerator overnight before testing the solution. The shear viscosity of the solvent mixture was calculated using values from literature and using the

assumption of the rule of mixture as shown below. This process was not further tested by measuring the viscosity of the solvent mixture.

$$\eta_{MeOH,23^{\circ}C} = 0.571 \text{ mPa}\cdot\text{s}$$

$$\eta_{CH_2Cl_2,23^{\circ}C} = 0.419 \text{ mPa}\cdot\text{s}$$

Solvent mixture: 75% CH₂Cl₂ and 25% CH₃OH

$$\begin{aligned} \eta_1(\text{viscosity of solvent}) &= 0.25\eta_{MeOH} + 0.75 \eta_{CH_2Cl_2} \\ &= 0.25 (0.71) + 0.75 (0.419) = \quad \mathbf{0.457 \text{ mPas}} \end{aligned}$$

Material	M _n [g/mol]	M _w [g/mol]	Polydispersity Index (PDI)	R _g (Radius of Gyration) [nm]
Società Acetate (SA)	27316	93978	3.4	17.4
Celanese UK (UK)	43634	98909	2.3	23
Celanese USA (USA)	42394	104228	2.5	23.2

Table 3.1 Materials Data from Gel permeation Chromatography (GPC) [23]

3.2 Experimental set up

3.2.1 Capillary Breakup Extensional Rheometer (CaBER)

The instrument used for the extensional rheometry is a HAAKE CaBER I form Thermo Electron Corporation designed by the Cambridge Polymer Group. It is made up of two end plates (with selectable diameters of 4mm, 6mm and 8mm), a Laser micrometer and Linear drive motor for moving

the upper plates. Temperature in the instrument is controlled by an external circulator which is connected to the CaBER I. The laser micrometer for the measurement of the diameter of the liquid fluid column has a resolution of $10\mu\text{m}$. The linear drive motor has a positional resolution of $20\mu\text{m}$. Figure 3.1 shows the CaBER I instrument. The separation of the plate can be done in three different ways; linear, exponential and cushioned stretches (Figure 3.2).

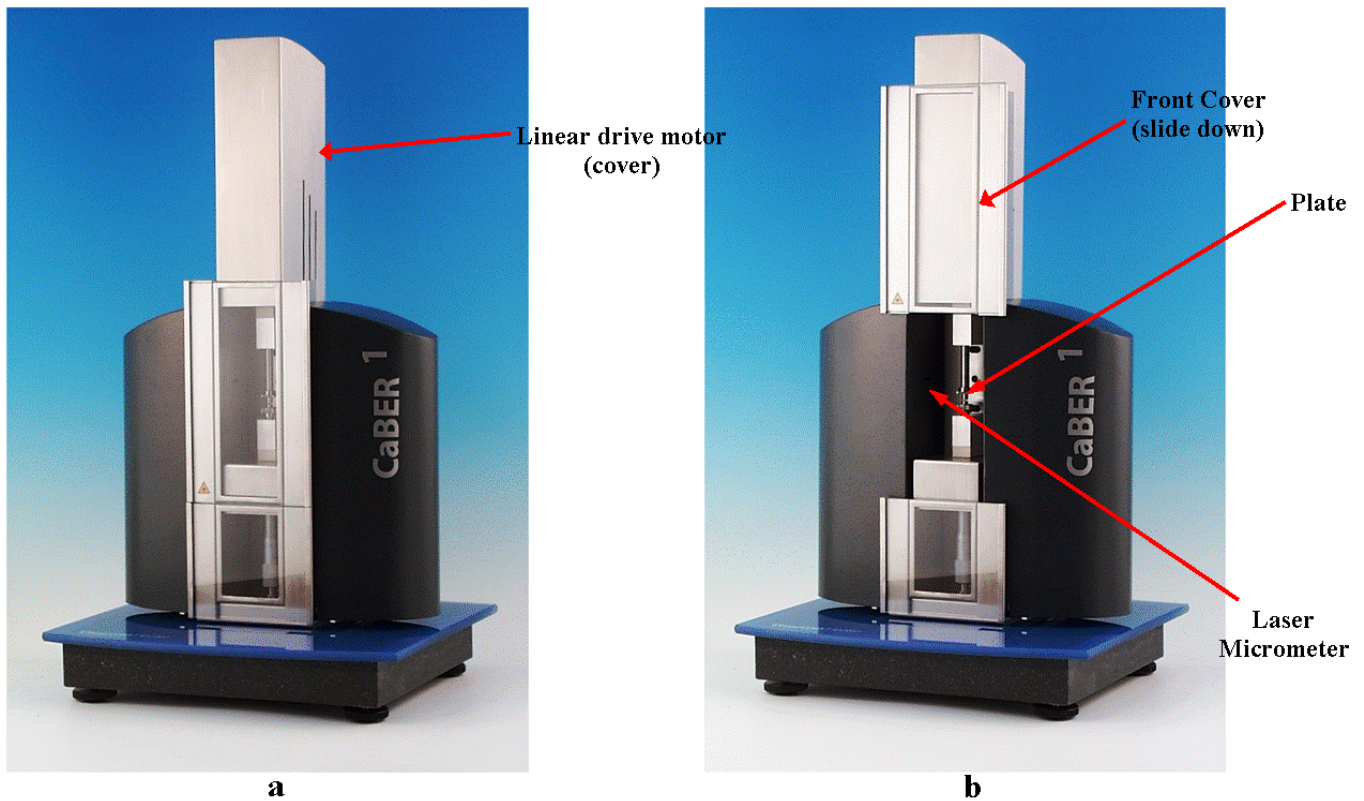


Figure 3.1 Picture of CaBER I, (a) Closed and (b) Opened

As can be seen from the literature survey of chapter 1, in performing capillary thinning experiments there are certain parameters that must be fixed or determined in order to have a good experiment, perform data analysis and extract useful material properties. These parameter include; the initial plate separation distance L_0 , final plate separation distance L_f , plate diameter D_0 , initial aspect ratio (L_0/R_0) and stretch ratio (L_f/L_0). The plate diameter will affect gravitational effect according to equation 12

(chapter 1) as increase in the plate diameter will increase the Bond number and also increase the sagging effect.

The optimal aspect ratio from simulations of filament stretching rheometry shows that, ratios in the range of $0.5 \leq \Lambda_0 \leq 1$ minimizes the effect of initial reverse squeeze flow, sagging and bulging of the cylindrical sample during stretching as stated by Rodd et al (2005) [20]. The final aspect ratios also affect the total instantaneous Hencky strain that is applied when the plates are separated [20]. The choice of the final aspect ratio for this work is from the previous work conducted in[24]. Throughout this project the values in Table 3.2 were used. It is observed that the initial aspect ratio falls within the range of 0.5 to 1 as stated by Rodd et al (2005)[20]. The stretch profile for this experiment is the cushioned profile; the reason being that there is reduction of problems due to fast deceleration and that is also a combination of the linear and exponential.

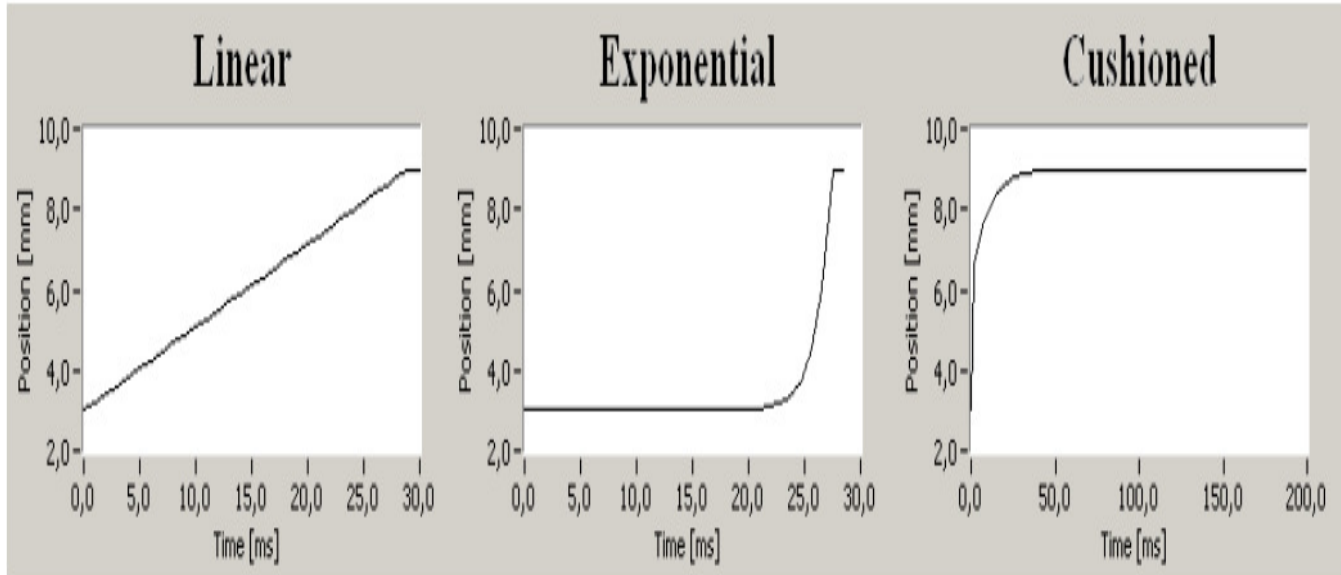


Figure 3.2 Stretch profiles [24]

D_0	6mm
L_0	2mm
L_f	10mm
Hencky strain	1.6
Initial Aspect Ratio ($\Lambda_0 = L_0/R_0$)	0.66
Initial Aspect Ratio ($\Lambda_0 = L_f/R_0$)	3.33

Table 3.2 Experimental parameters

The fluid samples are loaded with a syringe into the CaBER and the test performed immediately. The time taken for loading the sample is approximately 10 seconds. Test takes between 1 to 1.5 second to perform depending on the concentration, and the acquisition rate was 1000 Hz. The sample in the syringe is conditioned to test temperature in the bath of the external circulator of the CaBER I. The time elapsed before starting a new test campaign at any temperature is one hour to allow the sample to stabilize at the temperature. The experimental matrix is shown below

	Società Acetate (SA)			UK Celanese (UK)			USA Celanese (USA)		
	Concentration (%wt/v)								
Temp. (°C)	7	10	12.5	7	10	12.5	7	10	12.5
5									
10									
15									
20									

Table 3.3 Experimental matrix

3.2.2 Shear Rheometer

A Rheometrics DSR 200 rotational rheometer, equipped with cone and plate fixtures was used to measure the shear rheological behaviour of the cellulose acetate solutions. All tests were performed at room temperature. The rheological curves obtained are reported in appendix 4, and the main results described in the results part of this thesis.

3.2.3 Video Recording

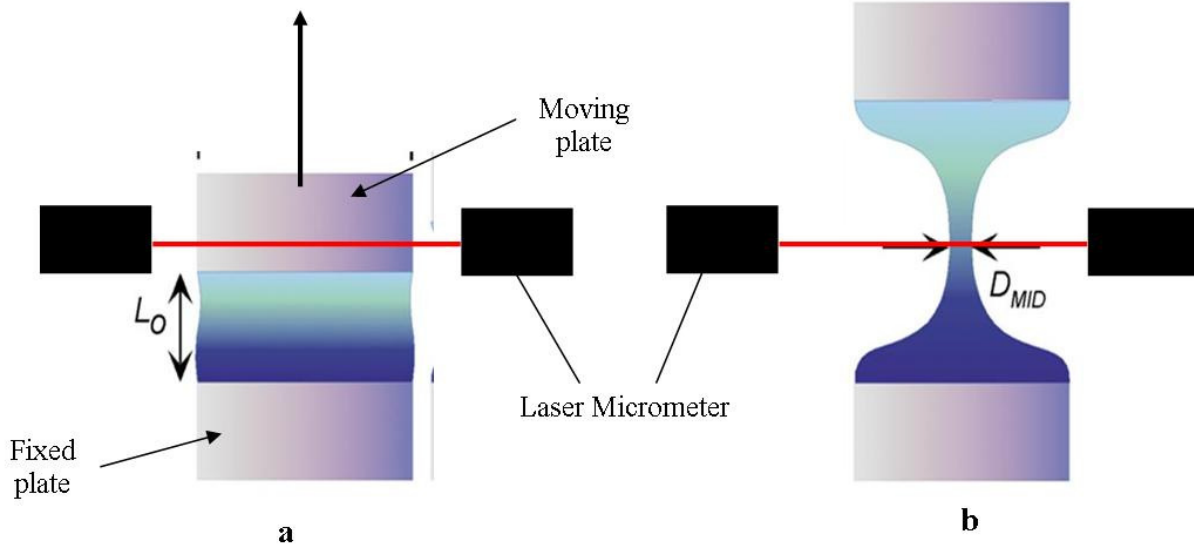
Video of the experiments were recorded using a MIKROTRON MC1310 high speed camera with a COMPUTAR MLH-10x 13-130mm lens at 300 and 1000 frames/seconds. The data were analysed using virtualDub and image J softwares. The videos were taken to observe the stretching process as well as the effect of evaporation on the test sample.

3.3 Data Analysis

The data from the CaBER software we analysed with Origin 8.0 software.

3.3.1 Determination of D_1 and D_0

The determination of D_0 and D_1 , the diameters before and after the stretching respectively are important for the extraction of material rheological properties as can be seen from table 2.1 and equation 21 (chapter 2). From the schematic diagram of the CaBER in sketch 3.1(a), it can be seen that the laser micrometer is not at the center of the fluid column diameter at the beginning of the experiment and therefore it cannot measure the correct diameter of the fluid cylinder D_0 .



Sketch 3.1 Schematic diagram of CaBER

We cannot simply assume that the initial diameter of the fluid column is the same as the diameter of the plate since it is possible to have under or over filled it and so the two diameters are rarely comparable. In figure 3.2(b), D_1 can be accurately determined by the laser micrometer if we are able to find the exact time when the upper plate stops moving. I am not all that convince about the D_1 value given by the machine since I do not know how it determines it.

From literature, Mckinley and Tripathi(2000) [2] stated a function that relates the D_0 , D_1 , L_0 and L_f (equation 26). Knowledge of D_1 or D_0 can be used to back calculate one from the other according to the formula. The initial and final heights are fixed and so knowledge of either D_0 or D_1 will help calculate one from the other. Videos were taken of the experiment to determine exactly when the plate stops moving so that D_1 could be determined.

$$\frac{D_1}{D_0} = \left(\frac{L_0}{L_f} \right)^{3/4} \quad (26)$$

A very good way of determining D_1 is to have video recordings of the experiment and measure the diameter, but this process requires that the machine be opened, with presence of lights and camera which can affect the experiment through evaporation. Also, the measurement of the diameter from the video will not be all that accurate since the exact point of the Laser on the diameter has to be estimated and the resolution of the videos should be taken into consideration, all these introduces a lot of errors. Therefore the video recordings were taken so we could link the time of stretching to a graph of strain rate versus time as calculated by the machine.

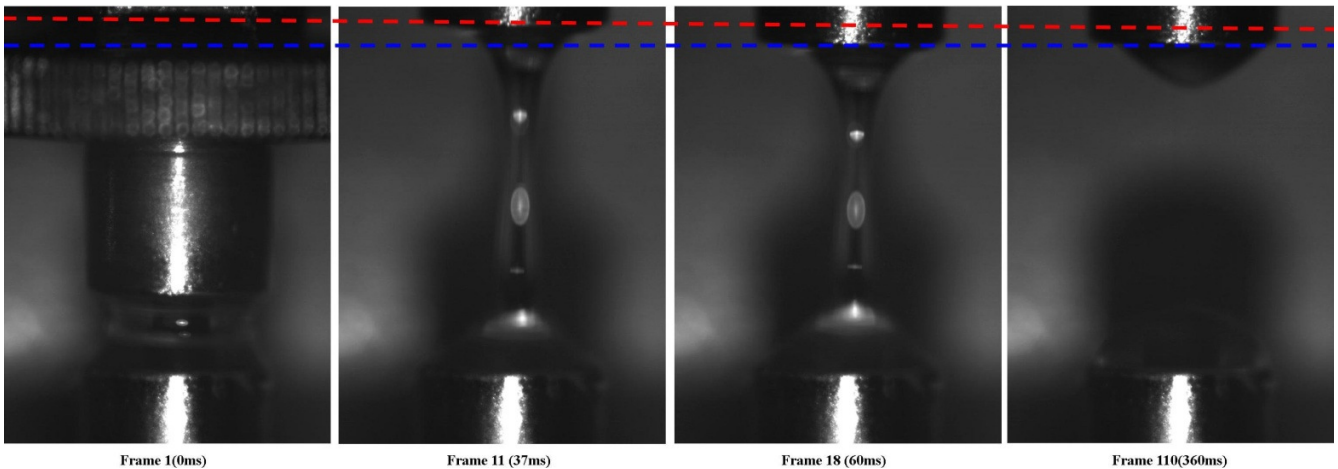


Figure 3.3 stretch profile from video recordings showing the highest extension and the final position of the moving plate (cushioned stretch)

The videos reveal that the plate moves up to a high stretch limit and then come down to the final stop (figure 3.3). The red line shows the highest point reached by the plate which later comes down to the final position (blue line).

These two times are marked on figure 3.4 reporting the strain rate measured. It was discovered that these two points are in the range of the lowest strain rates, therefore the point at which we have the lowest strain rate was arbitrarily taken to the point of seizure of the plate movement. The change in percentage of using the D_1 from the two times with reference to that from the machine is between 10 to

40% while the percent change between the two points with reference to the machine is between 4 to 8%.

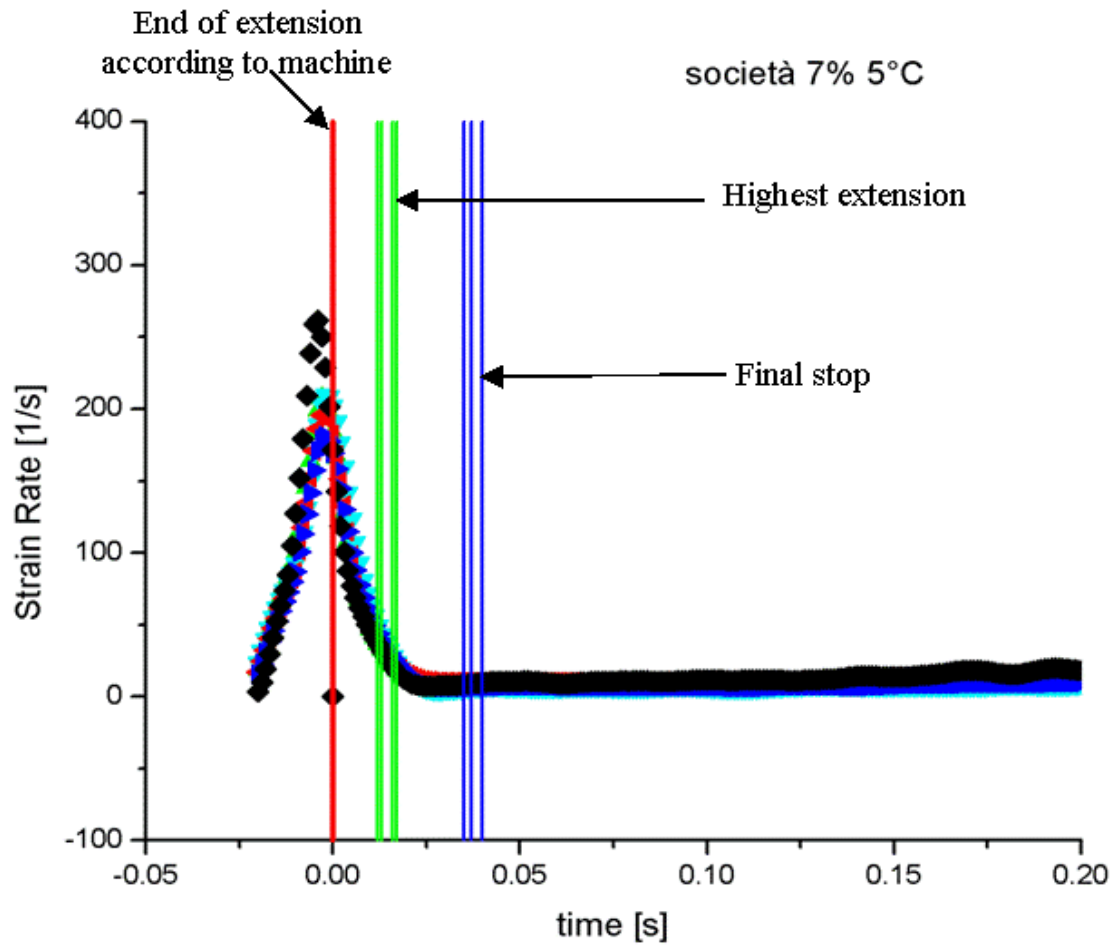


Figure 3.4 Plot of strain rate against Time from CaBER.

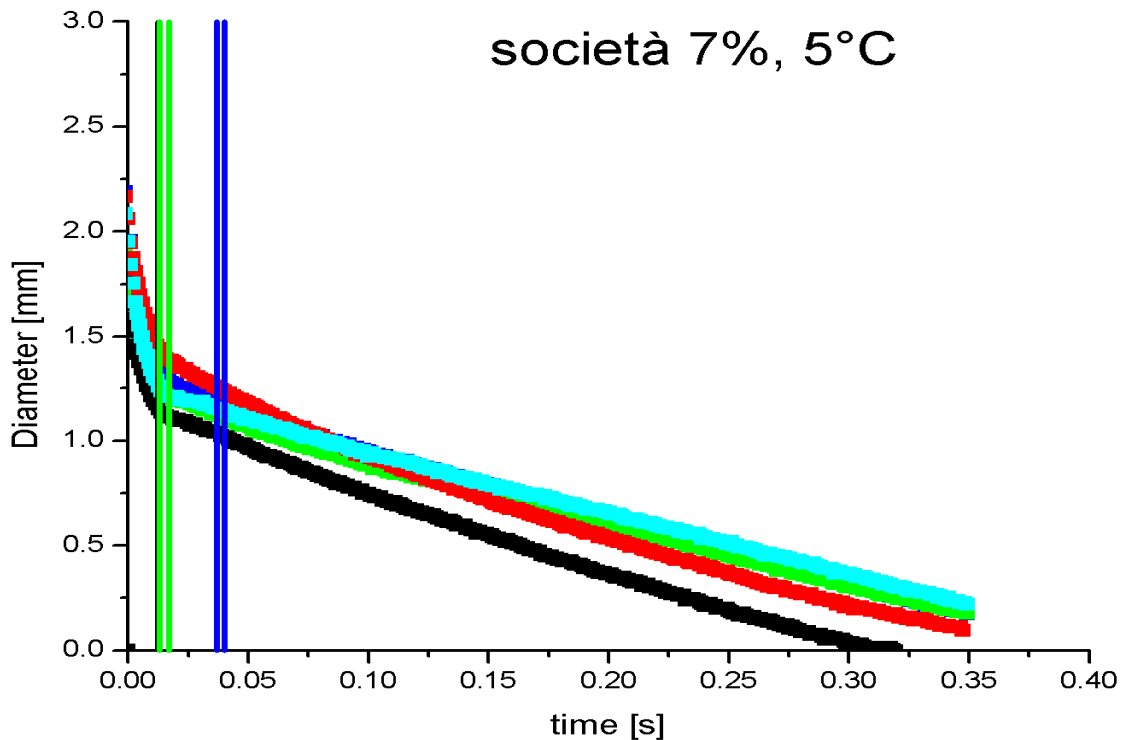


Figure 3.5 Diameter against time with the two times marked.

3.3.2 Apparent Viscosity determination

The Apparent Extensional Viscosity is defined by equation 20 (chapter 2), in this work it will be taken into account in order to predict the behavior of the system and ascertain the effect of concentration and temperature. The derivative in equation 20 is calculated in two ways by fitting the diameter versus time data to equation 21 from Anna and McKinley (2001) as shown in figure 3.6 and by a numerical method as illustrated in Sketch 3.2. The surface tension used is 30 mN/m because most polymer solutions have values around this, this was not verified for this particular solution.

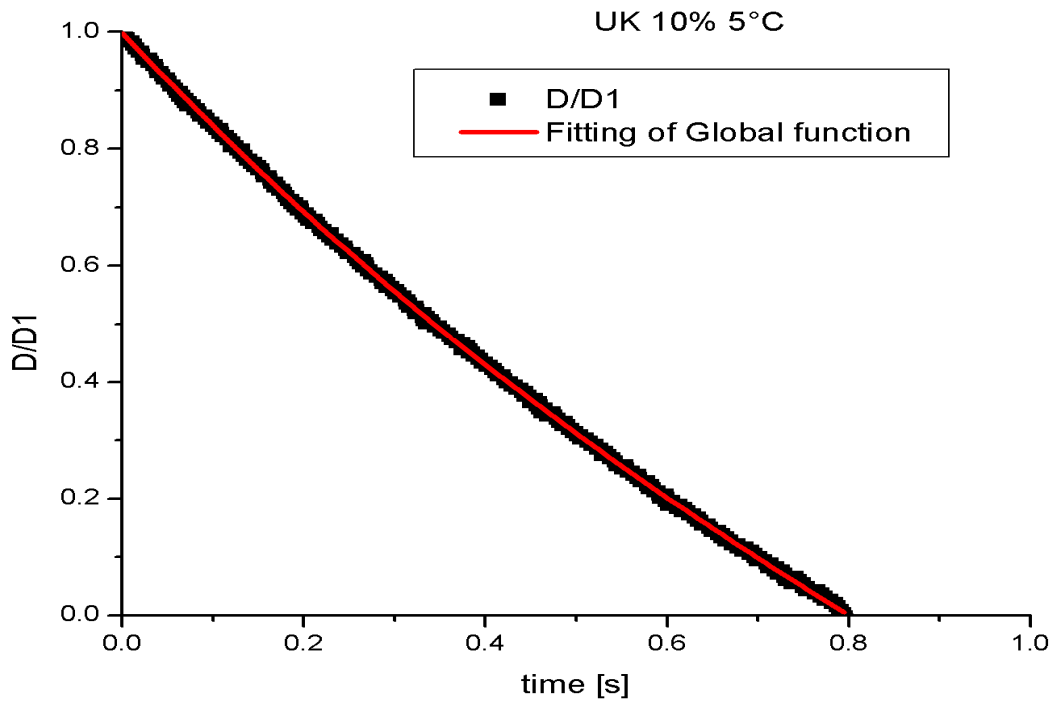
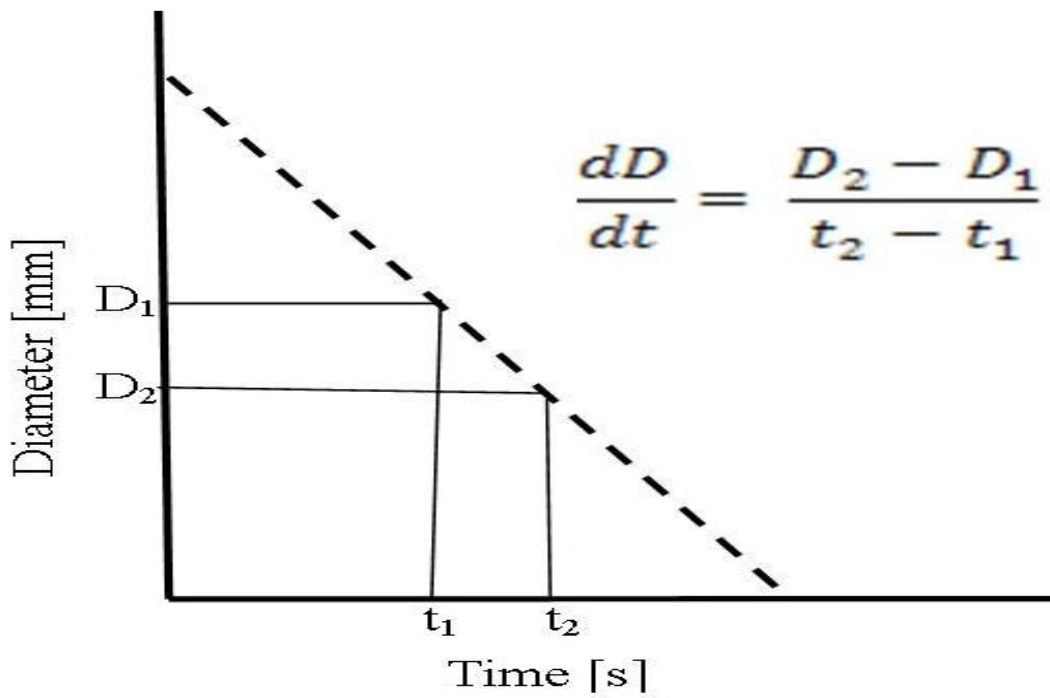


Figure 3.6 Fitting of global equation 20 to data



Sketch 3.2 Numerical calculation of derivative

Figure 3.7 shows the comparison between the results of the two methods. In the plot apparent extensional viscosity is reported as a function of Hencky strain, calculated by equation 11

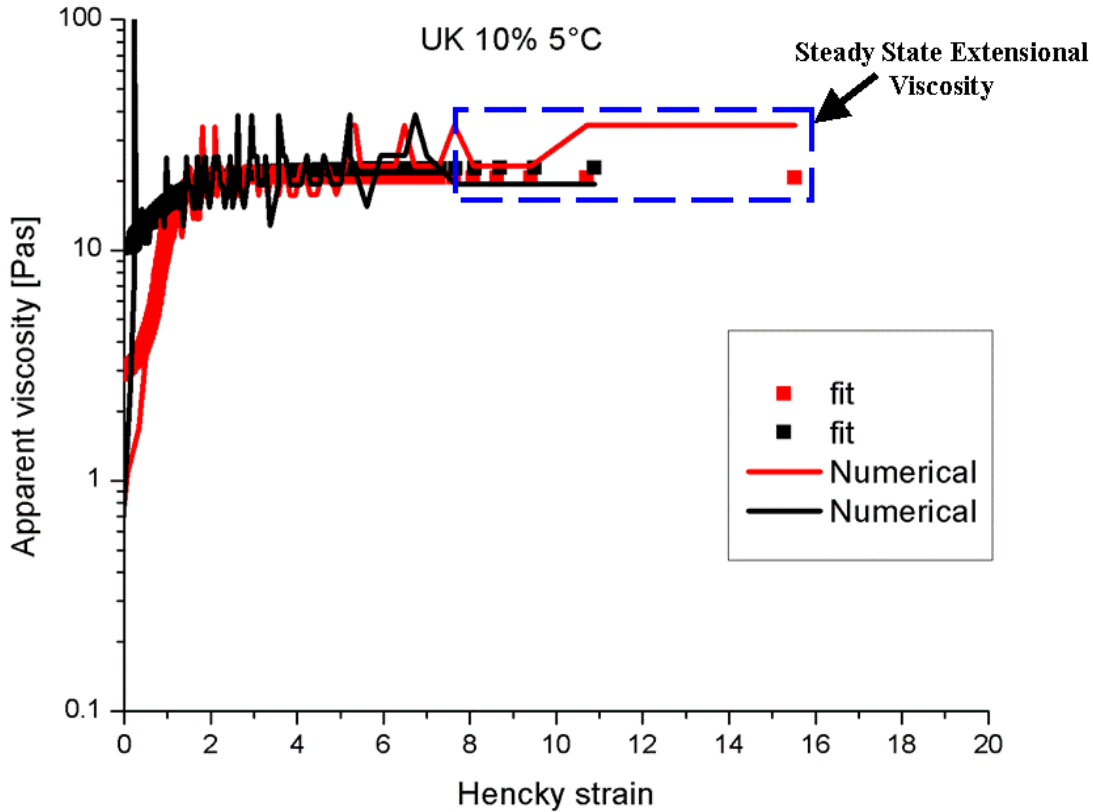


Figure 3.7 Apparent Viscosity versus Hencky strain as calculated using the fitting and numerical methods (line).

The numerical method gives a more noisy result than the fitting methods and this is related to a certain noise in the diameter readings versus time. Therefore the fitting to the equation were used throughout this project for calculation the apparent extensional viscosity. Finally, from figure 3.7 it is evident that the apparent extensional viscosity reaches a constant value, which suggest a Newtonian behaviour. In the following results and discussion, this observation will be motivated and effect of temperature and concentration on the apparent extensional viscosity and possibly spinnability will be discussed.

4.0 Results and Discussions

4.1 Diameter versus Time

The shape of the diameter versus time curve can be used to predict the behaviour of the fluid inspected. For the solution during this work the diameter of a Newtonian fluid should be linear. The normalised diameter versus time for my test solution is shown in figure 4.1

Figure

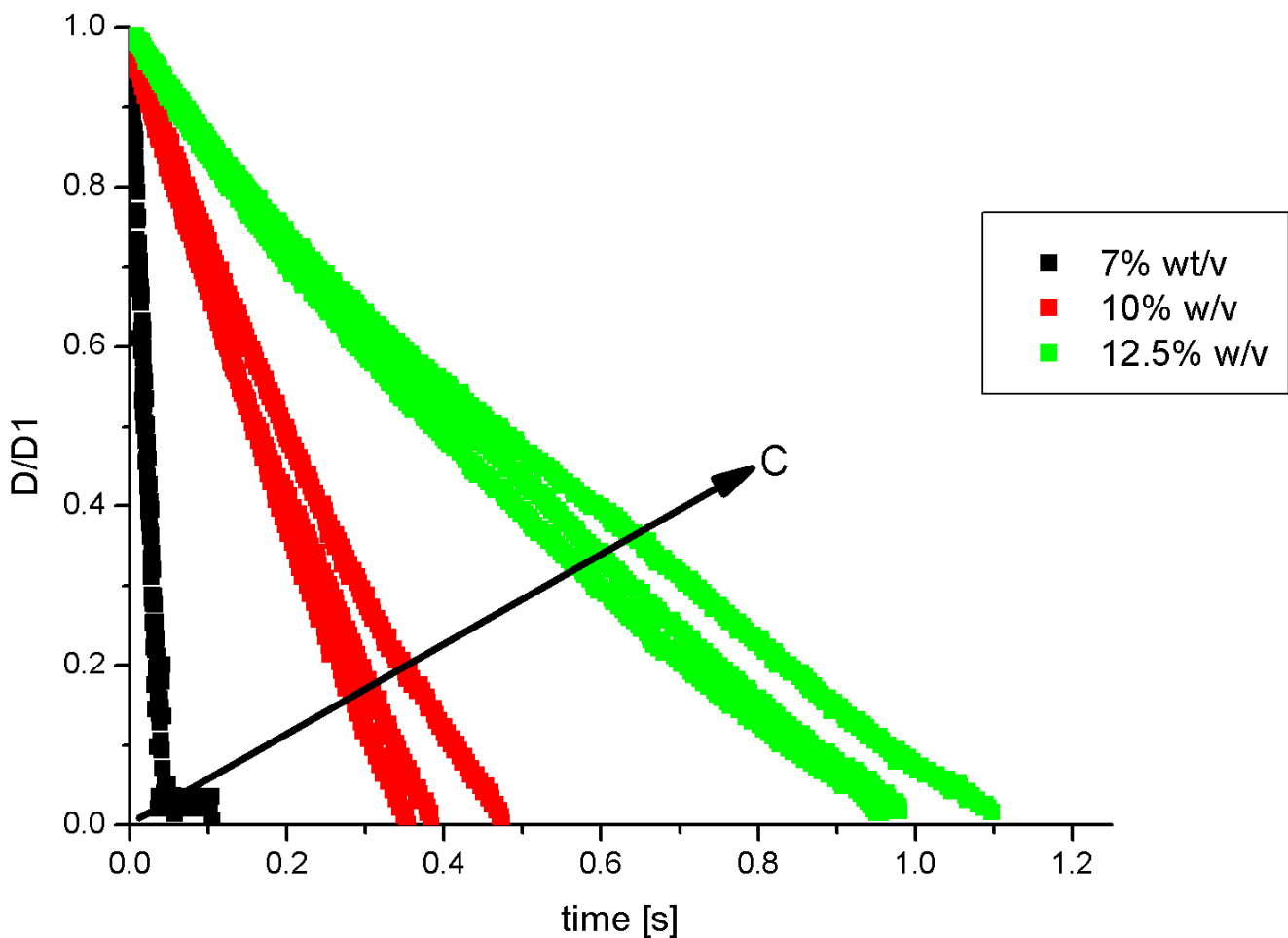


Figure 4.1 Normalised diameter versus time for S. solution with different concentrations and test temperature 5°C.

From the plot it can be seen that the diameter thins linearly and so the material display a Newtonian behaviour this has already has confirmed what already observed in stated in section 3.3.2 when the apparent extensional viscosity versus Hencky strain was observed to reach a constant value. On the other hand if the relaxation time of the solution can be calculated and then compare to the stretching time, we will be able to confirm this finding. The relaxation times for the polymer solutions used were calculated using

$$\lambda = \frac{1}{\zeta(v)} \frac{[\eta]\eta_s M_w}{RT} \quad (26)$$

where the prefactor $\frac{1}{\zeta(v)}$ according to Rodd et al (2005)[20] was given to be 0.463, R is the universal gas constant and T is temperature. The intrinsic viscosity was calculated using equations 5, 6, 7 in chapter 2 and from the empirical formula in equation 27

$$[\eta] = \frac{\phi_0 R_g^3}{M_w} \quad (27)$$

where ϕ_0 is a constant given to be $3.67 \cdot 10^{24} \text{ mol}^{-1}$, R_g radius of gyration and M_w is the molecular weight. Table 4.1 and 4.2 shows values of the intrinsic viscosity calculated.

		Martin's Equation		Huggin's Equation		Kraemer's Equation	
	Equation(27)	$[\eta]_M$ dl/g	K_M	$[\eta]_H$	K_H	$[\eta]_K$	K_K
SA	2.057	6.905	0.02	-	0.006	1.502	0.036
UK	4.515	8.741	0.016	-	0.004	1.6	0.034

Table 4.1 Intrinsic viscosity calculated using viscosities from shear rheometry

Material		Martin's		Huggin's Equation		Kraemer's Equation	
	Equation(27)	$[\eta]_M$	K_M	$[\eta]_H$	K_H	$[\eta]_K$ dl/g	K_K
SA	2.057	81.83	0.002	-3745	4.30E-05	1.664	0.024
UK	4.515	60.81	0.003	-6457	2.32E-05	1.66	0.023
USA	4.397	46.38	0.003	7063	1.98E-05	1.621	0.023

Table 4.2 Intrinsic viscosity calculated using steady state extensional viscosities

The relaxation times were then calculated using equation 26 with the highest intrinsic viscosity value (Martin's equation) shown in Table 4.3.

Material	Relaxation time [ms]		
	Equation 27	Extensional Viscosity	Shear Viscosity
SA	0.002	0.066	0.0056
UK	0.004	0.052	0.0074
USA	0.004	0.042	

Table 4.3 Relaxation times for all three materials

It is observed that the relaxation times are much less than the experimental time needed for stretching (approximately 50ms); therefore during the stretching the polymer should have fully relaxed and so we will not observe the relaxation during thinning. This reason accounts for the linear behavior of the diameter versus time curve which seems to be changing with increase in concentration. The entire diameter versus time graphs for all materials are presented in Appendix 1.

4.2 Effect of Temperature

4.2.1. Apparent Extensional Viscosity

For polymeric materials, the effect of temperature on the viscosity can be of Arrhenius type i.e. viscosity is expected to decrease with increasing temperature or according to the Williams-Landel-Ferry (WLF) equation. The plot of temperature versus steady state extensional viscosity is shown in figure 4.2 for various concentration of the materials studied. The apparent extensional versus Hencky strain graphs have been presented in Appendix 2.

Steady state Extensional viscosity vs Temperature

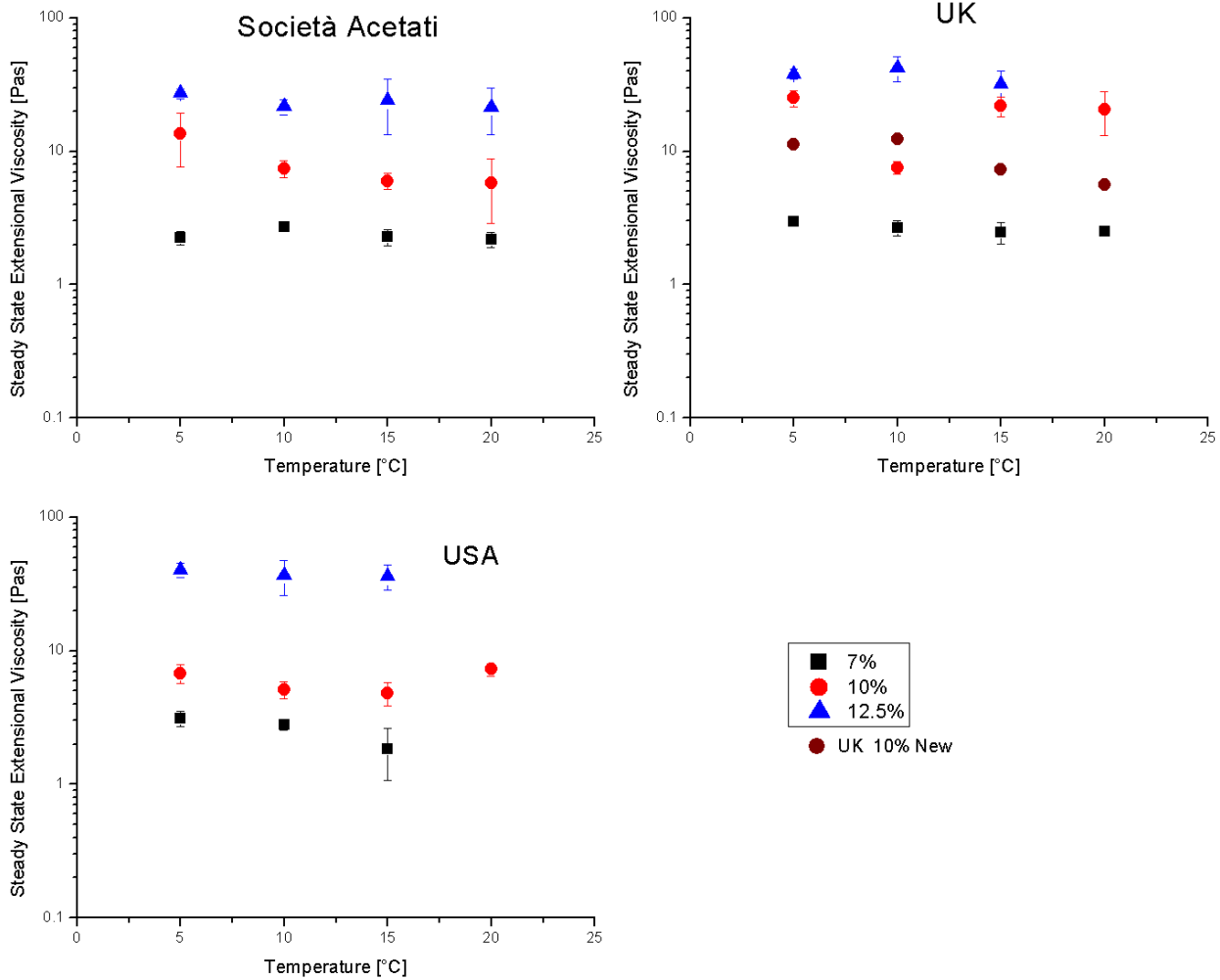


Figure 4.2 A plot of Steady State Extensional Viscosity with temperature.

Apparently, it is difficult to determine the dependence of steady state extensional viscosity on temperature for this particular system, as in some one instance there is the decrease of viscosity with temperature, in some other an unexpected increase and in others there seems to be no effect at all. There is no effect of temperature on the steady state extensional viscosity for all materials at 7% wt/v concentration while there is a sort of dependence for the 10% and 12.5% concentrations. Conversely results from a solution of cellulose acetate in ethyl lactate shows the expected Arrhenius dependence on temperature (figure 4.3) [24].

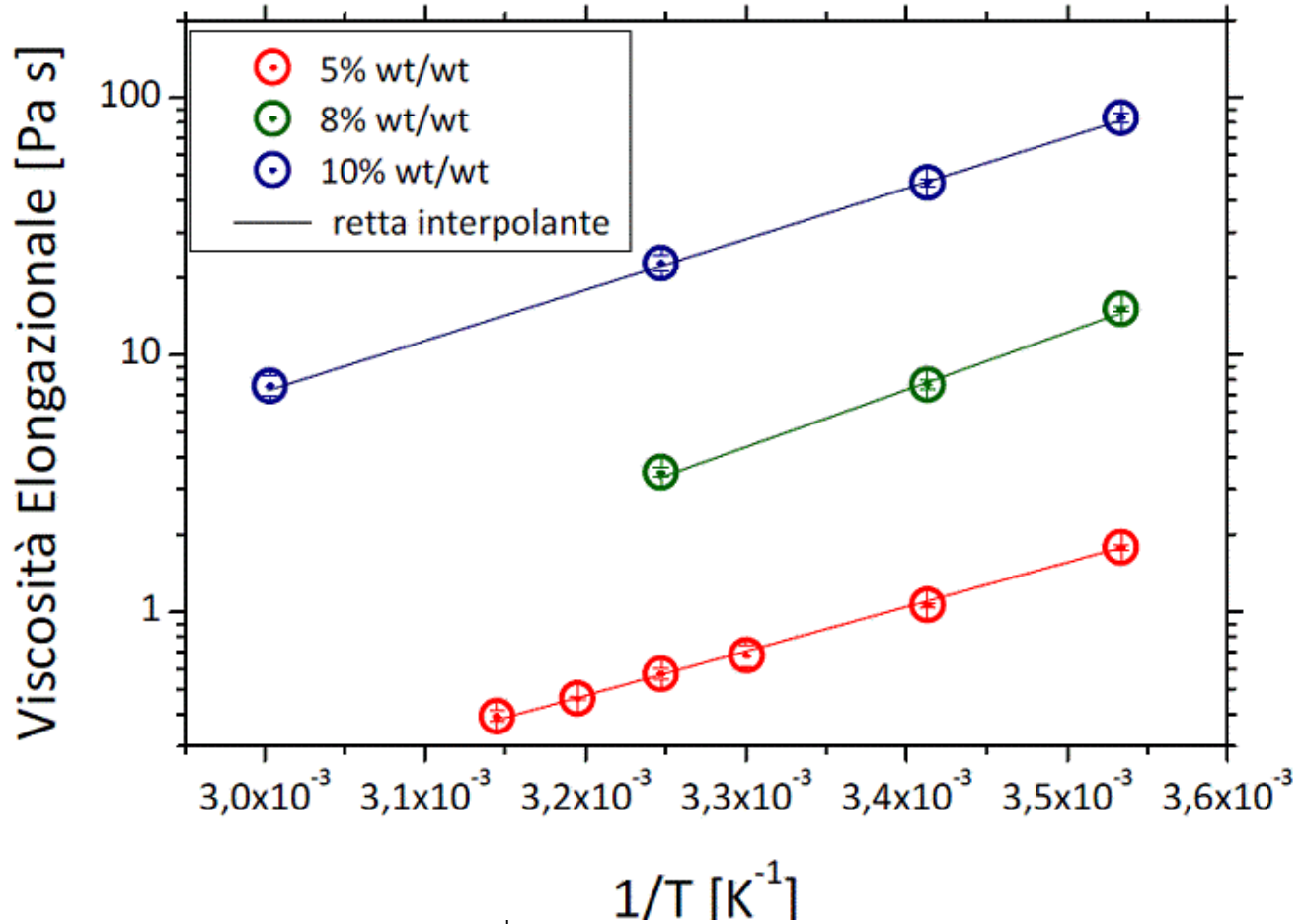


Figure 4.3 extensional viscosities with T^{-1} showing Arrhenius behavior for a cellulose acetate solution of concentrations 5%, 8% and 10%. [24]

This discrepancy we suspect to be the effect of solvent evaporation. To check this hypothesis, a series of experiments were carried out after a defined elapse of time from loading the sample. The tests were video recorded. These experiment were conducted with a 7% wt/v concentration at 5°C and the waiting times were 30, 60, 120, 180 and 300 seconds. From the videos, there is the formation of a skin on the liquid bridge surface which during the stretching period may break to reveal the liquid inside.

Figure 4.4 shows images from the videos of a “skin” formed on the surface. Wee and Mackley (1998) [25] also observed the formation of “skin” on a cellulose acetate in acetone due to evaporation. The skin was observed to have affected the experiment by causing an increase in both the storage and loss moduli. This confirms that solvent evaporation can happen during the test especially at higher

temperatures and this can cause concentration of the solution and also increase the apparent viscosity. Also the time of conditioning the solution before testing can cause increase in concentration through evaporation.

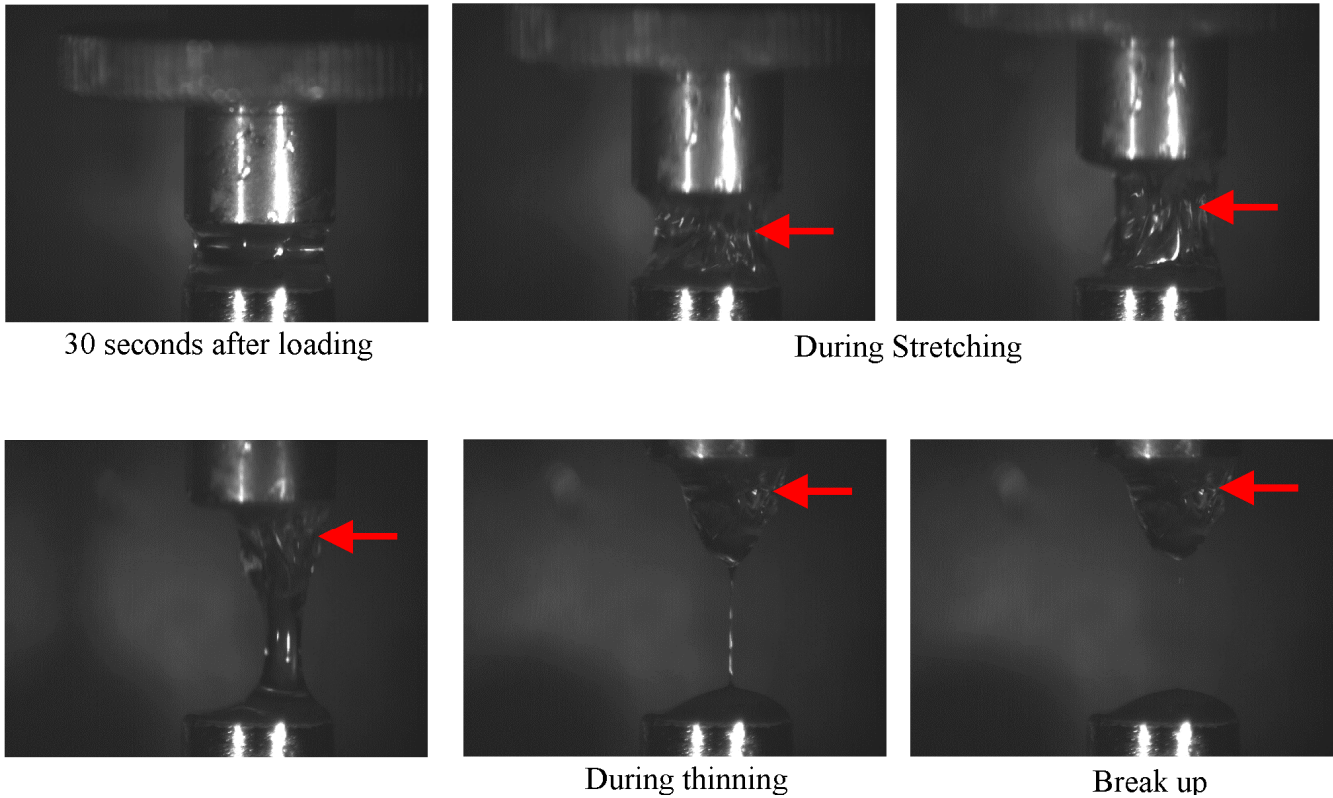


Figure 4.4 Images from video recordings showing the skin formed on the fluid column (red arrow).

Moreover, during the stretching the skin will break, then we observe a decrease in the time to break resulting from a lower D_1 as can be seen in the figure 4.5. In some cases, evaporation occurred in the whole sample; in this case the sample behaves as a very viscous fluid with long time to break. Of course this phenomenon prevents determination of a meaningful extensional viscosity as well as a significant time to breakup.

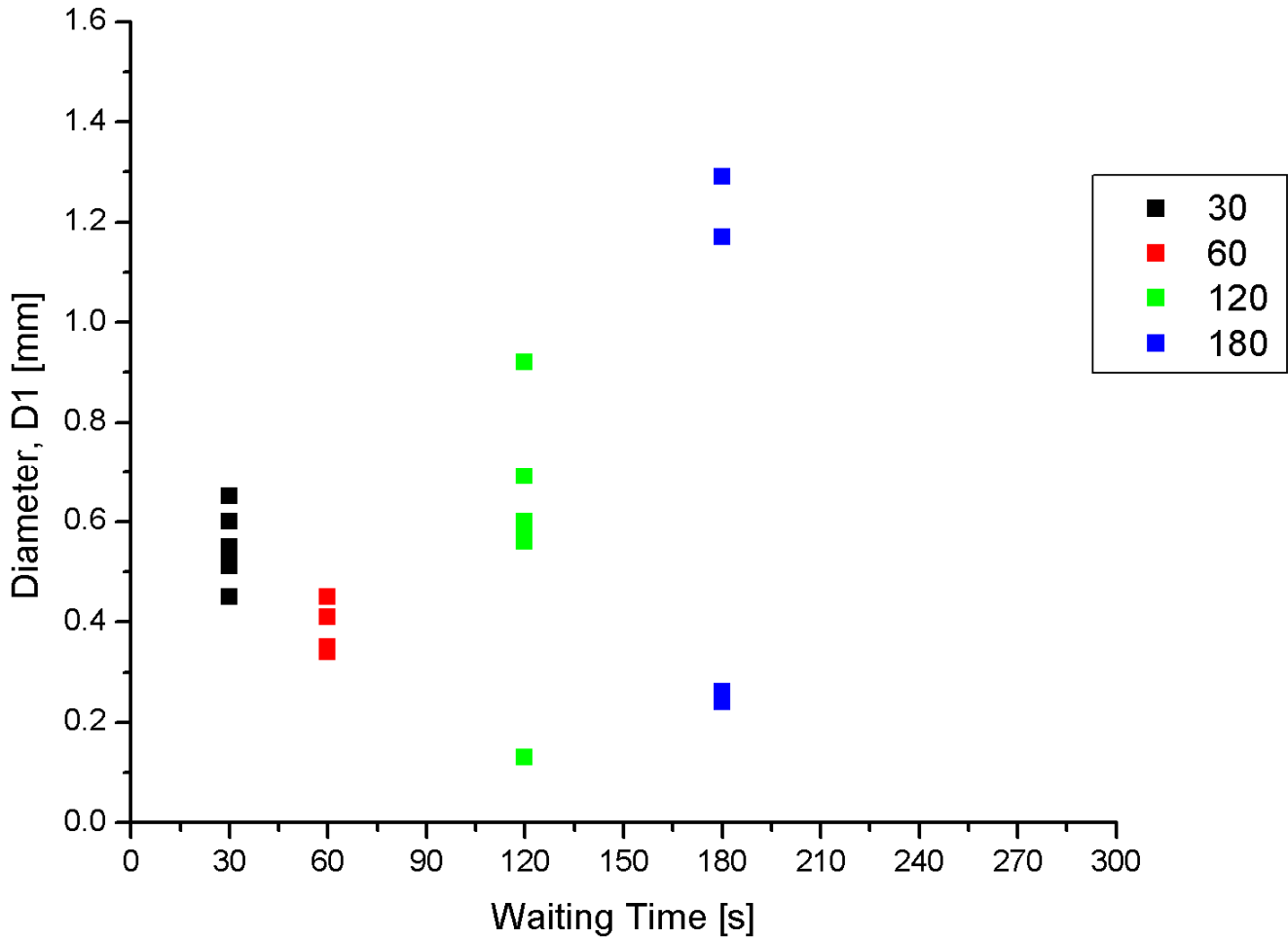


Figure 4.5 Diameter (D_1) versus waiting time

4.2.2 Time to Break up

The time to break up of a polymer fluid is an important processing parameter according to [11] which relates to fluid properties and geometry of the liquid bridge. Also, Wang et al (2004) [19] used the time to breakup of Poly (MMA-CO-MAA) copolymers to predict the spinnability of the solution to form uniformed fibers. In their paper, a higher time to breakup was related to good spinnability as against these with a lower time to breakup. According to Rodds et al (2005) [20] the characteristics time to breakup (t_v) for a Newtonian fluid when gravitational effect is neglected can be given by $t_v = 14.1\eta_s R_0 / \sigma$, which shows that this is governed by the fluid viscosity (η_s) and the surface tension (σ).

Conversely the time to break up of a fluid jet into droplets is defined by the Rayleigh time scale (t_R) given by

$$t_v = \sqrt{\rho R_0^3 / \sigma} \quad (28).$$

The ratio of the viscous time scale (t_v) and the Rayleigh time scale (t_R) is a dimensionless time scale called the Ohnesorge number (Oh). This can be used to determine if during extension the fluid will thin into a filament or give rise to the formation of droplets. Also Chang et al (2008) [21] used another dimensionless number; the Deborah number to determine the formation of bead-on-string structure or uniform fibers of a cellulose acetate solution. The Deborah number (De) is the ratio of the polymer relaxation time (λ) to the Rayleigh time scale;

$$De \equiv \frac{\lambda}{t_R} = \frac{\lambda}{\sqrt{\rho R_0^3 / \sigma}}. \quad (29)$$

The time to breakup against temperature is shown in figure 4.6.

Time to Break up vs Temperature

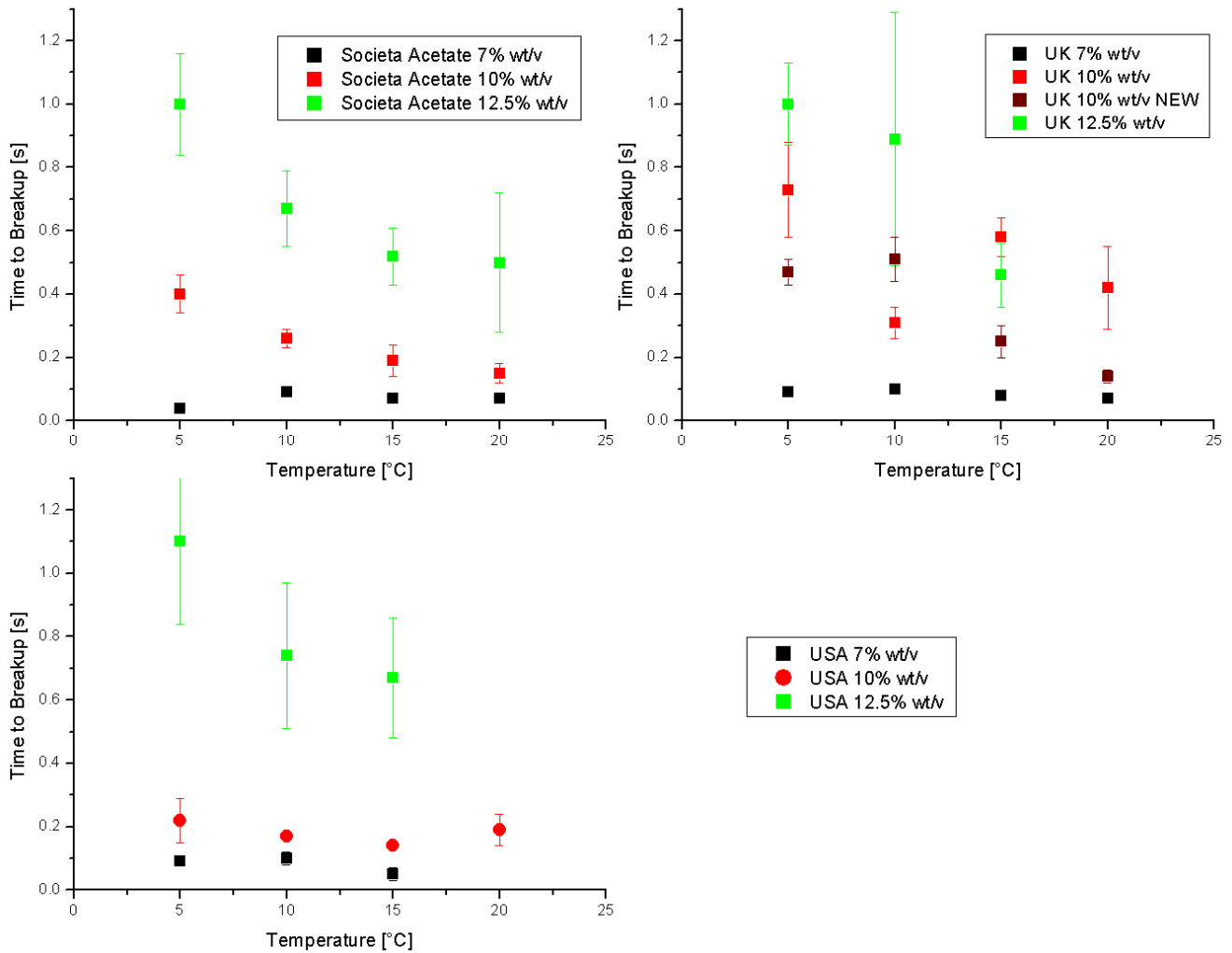


Figure 4.6 Time to break versus Temperature for all materials. The relevant diameter vs. time curves is in Appendix 1

The time to break differs for each material type, concentration and temperature. The time to break for SA-7, UK-7 and USA- 7 does not depend on temperature. For the 10% wt/v concentration all the three shows significant difference. SA shows a decrease in time to break for increasing temperature. The observation for UK is different showing a increase in time to break from 5°C to 10°C then a decrease a for 15°C and 20°C. we could not explain this behavior and we couldnot even explain the different

behavior of different batches reported in UK and UK New. USA also shows a decrease in time to break with increasing temperature up to 15°C, followed by an increase.

It is observed also that the time to break increases with increasing concentration, therefore the increase in time to break with temperature can be as a result of evaporation thereby increasing the concentration which causes a further increase in time to break up. In all three materials, it is observed that as the temperature increases, the curve tends to be more dispersed which we suspect to be the effect of evaporation and the formation of a skin on the fluid surface as Figure 4.4 above

4.3 Effect of Concentration

4.3.1 Time to Break up

The effect of concentration on the time to break for all material is greatly evident from Table 4.4 which shows the relative change in viscosity for moving from one concentration to another for all materials. For example for a temperature of 5°C changing the concentration from 7% to 10% wt/v for SA increases the time to break up almost 900%, and similar results are obtained for all temperatures. Figure 4.7 shows a plot of time to break up against concentration in all materials and at all temperatures.

Società Acetate	Viscosity [%]				Time to Break up [%]			
Concentration Effect	5°C	10°C	15°C	20°C	5°C	10°C	15°C	20°C
7 – 10	+500	+174	+163	+165	+900	+189	+171	+114
10 – 12.5	+101	+190	+302	+269	+150	+158	+174	+233

Table 4.4 Relative change in time to breakup and Steady state extensional viscosity for SA, (+) means increase and (-) decrease. Appendix 3 has tables for all other materials.

Time to break up vs Concentration

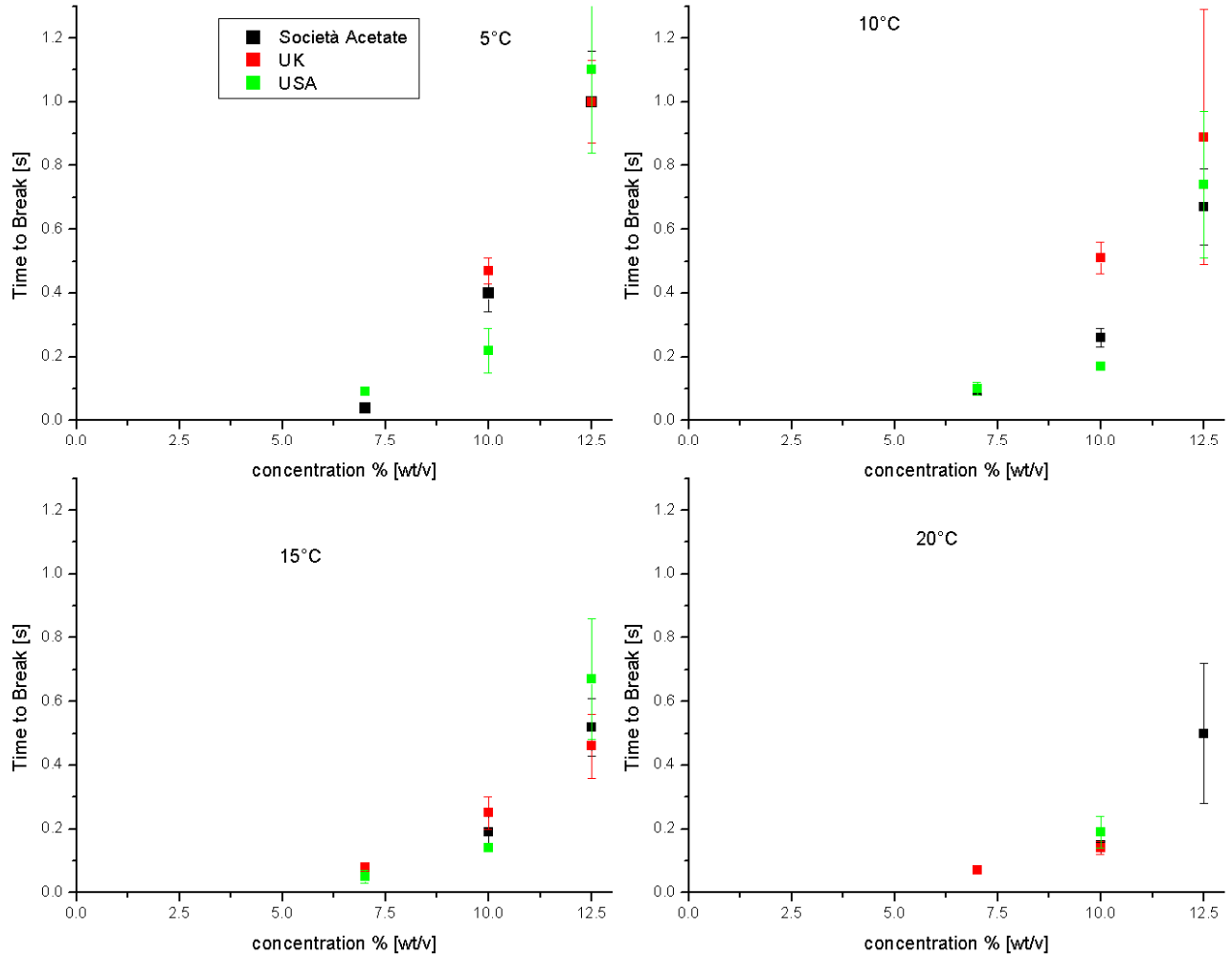


Figure 4.7 Time to Break up versus concentration.

There is an increase in the time to break, suggesting that an increase in concentration favours the thinning process and therefore spinnability with respect to drop formation. This can be the result of the increase in entanglement as concentration increase breaking process and therefore of the increase in the friction of the entangled chains which retards the thinning process. The same effect was observed by Wang et al (2004) [19] upon the inclusion of clays into copolymer of methyl methacrylate (MMA) and methacrylic acid (MAA) decreased the capillary thinning and increased time to breakup. This according to the paper is as a result of increase in the zero-shear rate viscosity but did not explain it based on the structure of the solution.

The critical concentrations for all materials were calculated by equation using equation 30

$$c^* = \frac{0.77}{[\eta]} \quad (30)$$

The intrinsic viscosities in this calculation is the shear flow viscosity showed in Table 4.1. In extensional flow according to Clasen et al (2006) [25] this value should be lower which was stated as $0.1c^*$. The results show that the concentration we are using this study is above the critical concentration and so the power law dependence is justified Table 4.5.

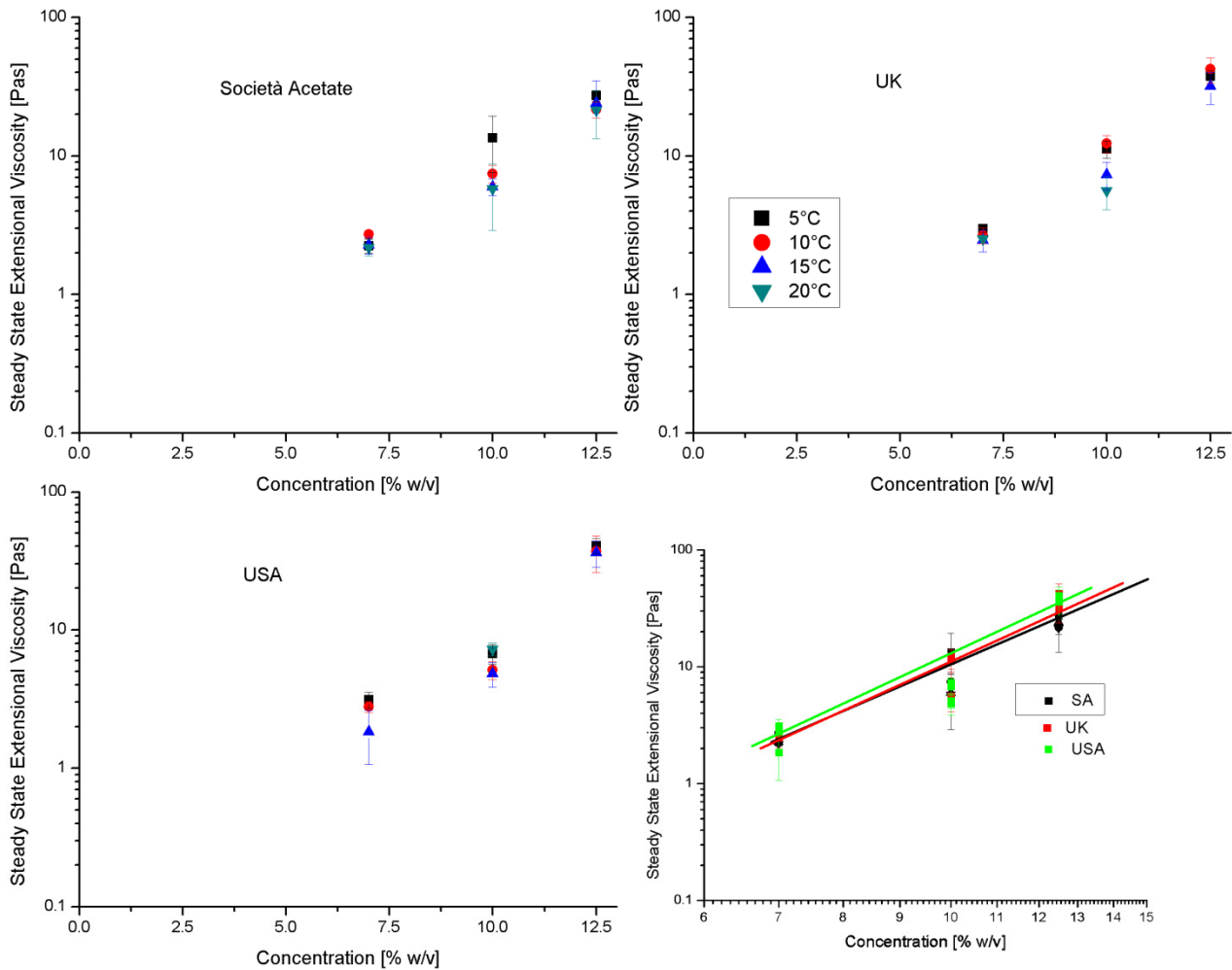
Materials	Critical Concentration, c^* (%w/v)		
	Equation 27	Martin's Equation	Kremer's Equation
SA	0.3743	0.1115	0.5126
UK	0.1705	0.0881	0.4813
USA	0.1751		

Table 4.5 critical concentration of solutions

4.3.2 Steady State Extensional Viscosity

The effect of concentration on the steady state extensional viscosity is as remarkable as in the time to break. All materials show an increase in steady state viscosity with concentration which confirms the increase in entanglement of polymer chains with concentration thereby increasing the resistance during flow. Figure 4.8 show a plot of the steady state extensional viscosity with concentration

Steady State Extensional Viscosity vs Concentration



Lines drawn by hand not fitting

Figure 4.8 Steady state extensional viscosities with concentration

A power law dependence on concentration was observed by Ji-Huan et al (2008) [22] on the shear viscosity of Polyacrylonitrile in N,N-dimethylformamide (DMF) in the form of $\eta \propto c^\beta$ where β is the power law index.[20] The shear viscosity of two of the solutions used in this project is presented in figure 4.9 versus concentration and shows a power law dependence. The power law indexes for the two materials (SA and UK) are the same with a value of 2.9. The difference in the materials is the constant of proportionality which shows that the viscosity at any concentration is higher in UK than SA.

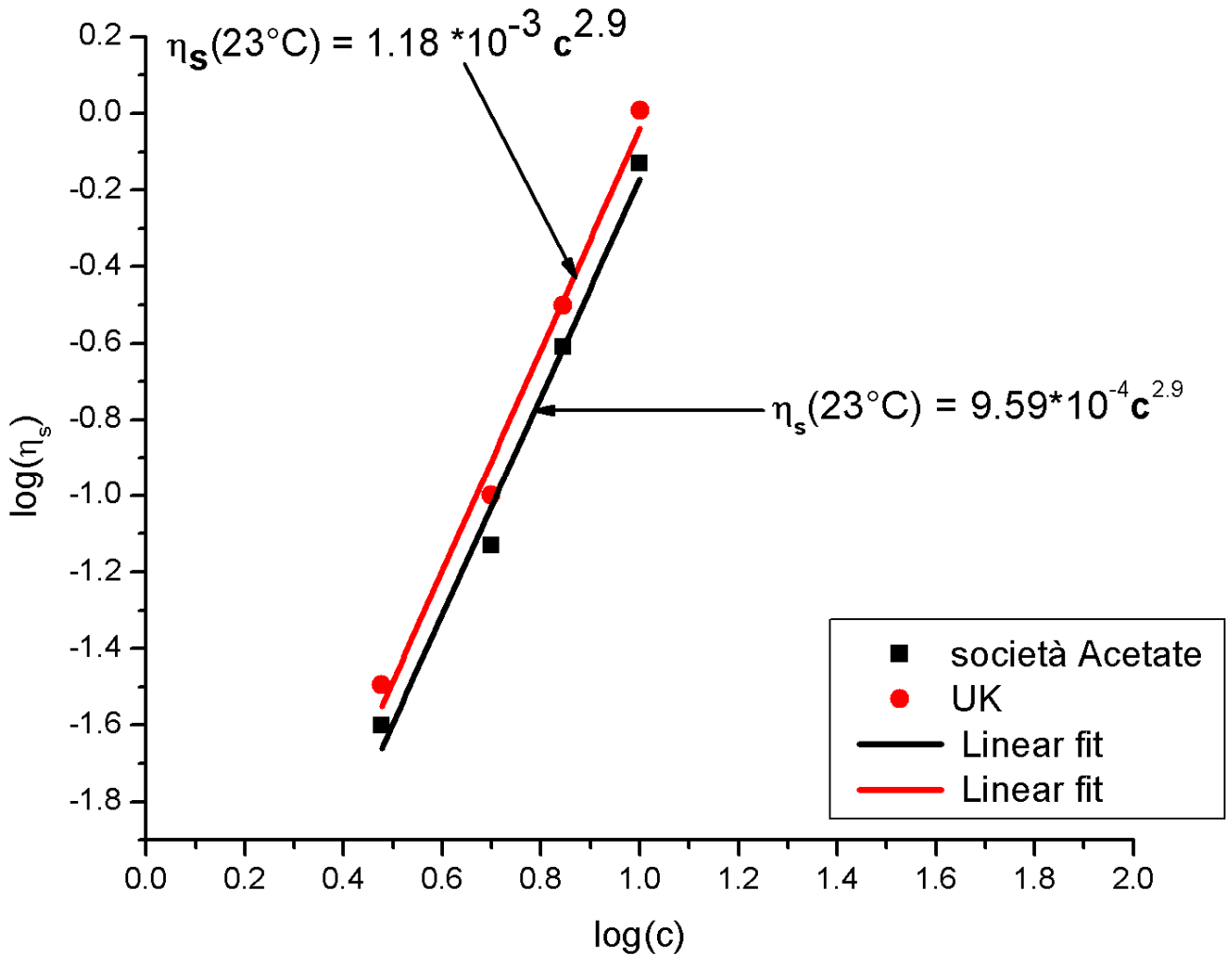


Figure 4.9 shear viscosity vs. concentration of cellulose acetate in dichloromethane/methanol (75/25)

A similar plot for the steady state extensional viscosity versus concentration is plotted in figure 4.10. The power law indexes are shown on the graph. UK and USA shows similar index of 4.4 as against SA which shows a lower value of 3.9. As compared to the shear viscosity, the extensional viscosity shows high values.

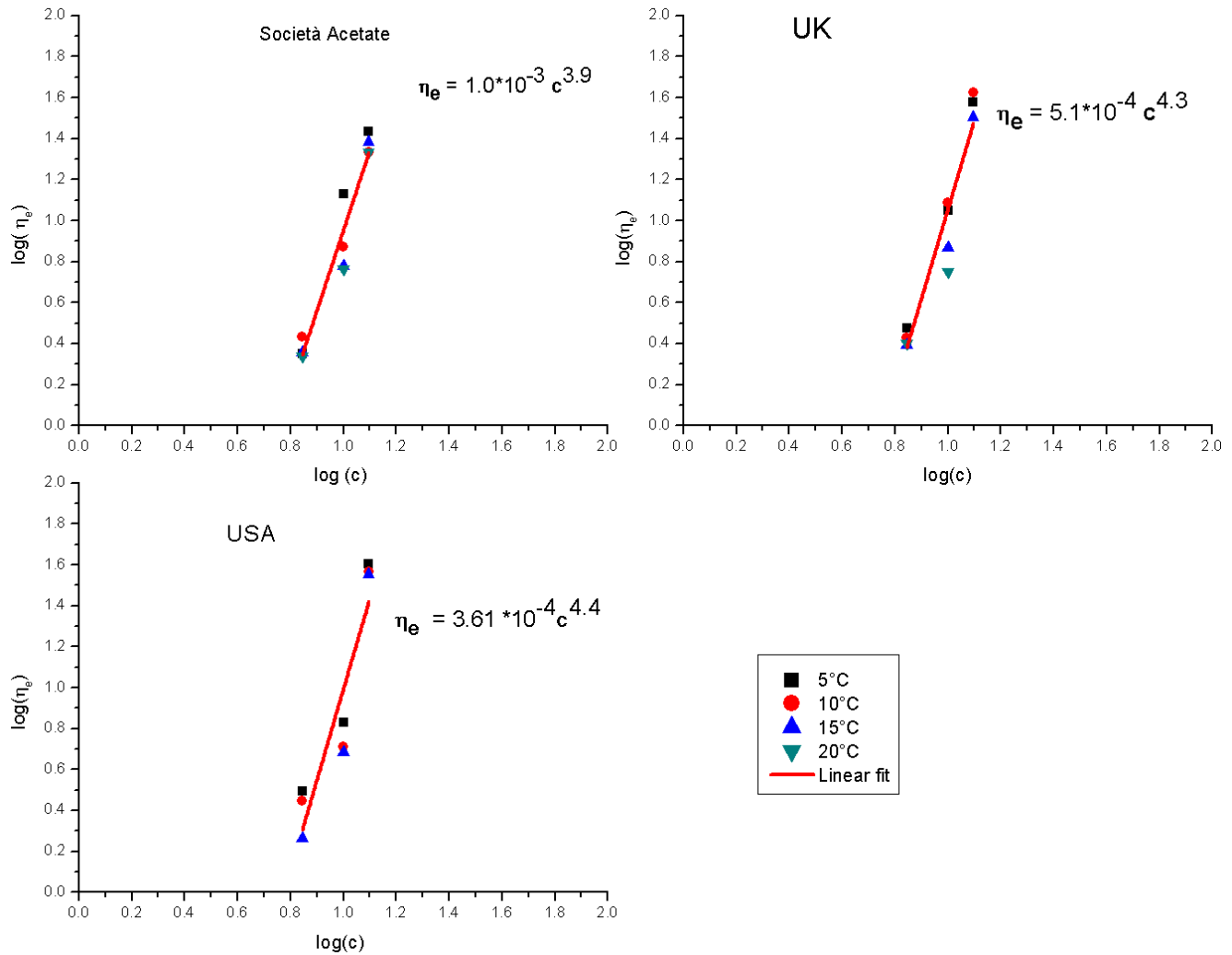


Figure 4.10 Steady state Extensional viscosities vs. concentration of cellulose acetate in dichloromethane/methanol mixture

4.4 Time to break up and Steady state extensional viscosity

As it has been observed above, the time to break up of the liquid bridge can be used to determine the processability of the solution because it gives the time allowed to process the materials before there is a break up. On the other end, this quantity should be affected by the fluid extensional viscosity which opposes the action of surface tension and slows down the thinning phenomenon. [1]. Therefore, when the thinning process is linear we expect that a graph of time to break up against steady state extensional

viscosity should also be linear. Figure 4.11 presents all the available data on the time to break up versus extensional viscosity.

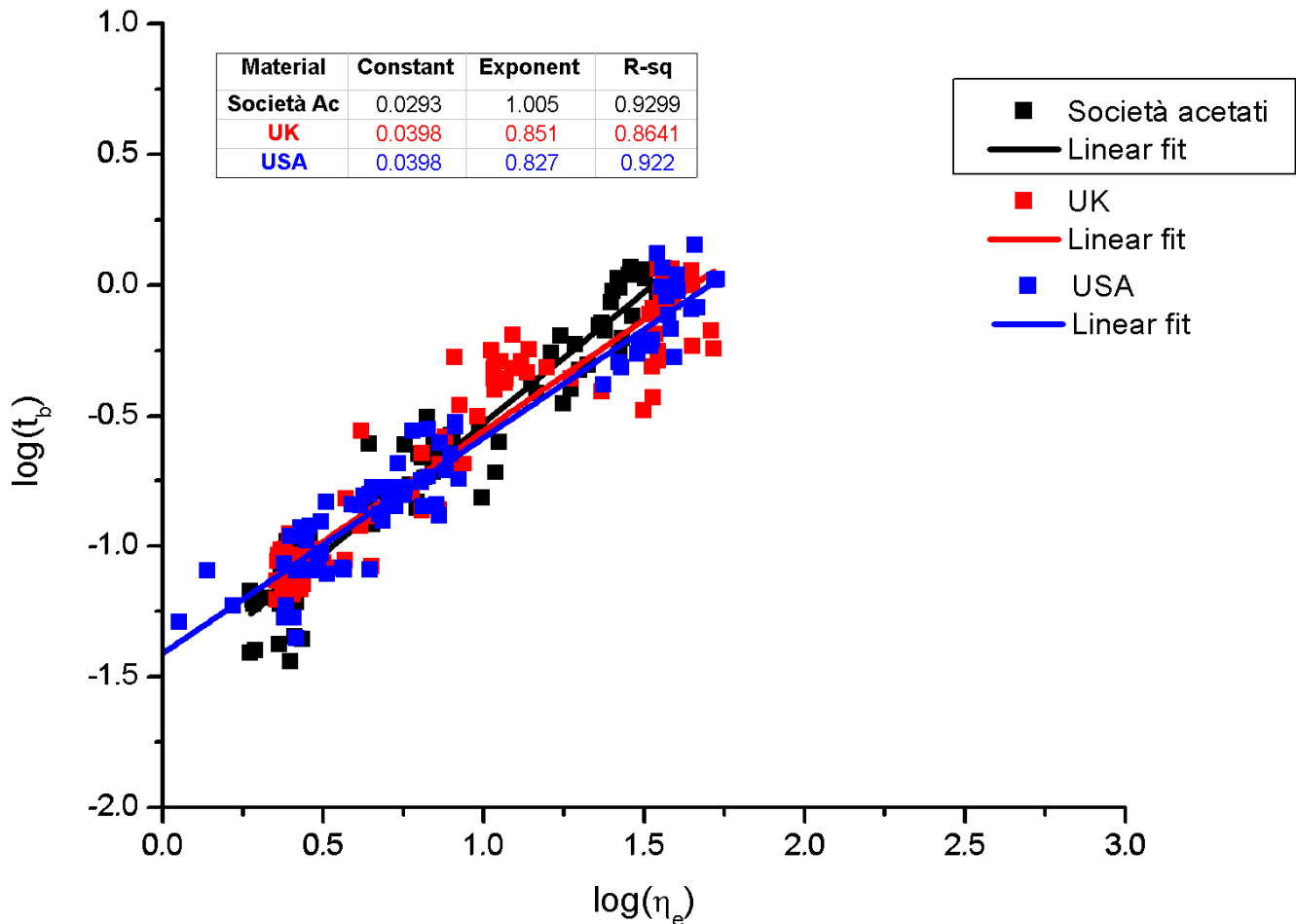


Figure 4.11 time to break up (t_b) vs. steady state extensional viscosity (η_e)

It should be observed that a good correlation exist irrespective of concentration and temperature. This relationship seems to be linear for SA, whiles UK and USA show power law dependence with an index of 0.851 and 0.827 respectively. Again, UK and USA have similar dependence as compared to SA. This relationship can be used to predict the behavior of the solution as to the nature of the diameter versus time curve for a particulate solution or system. Attempts have also been made to derive an expression for the time to break up in terms of the concentration of the solution by combining the expressions for η_e in terms of c and t_b with η_e , the results of which are presented in equation 31,32 and

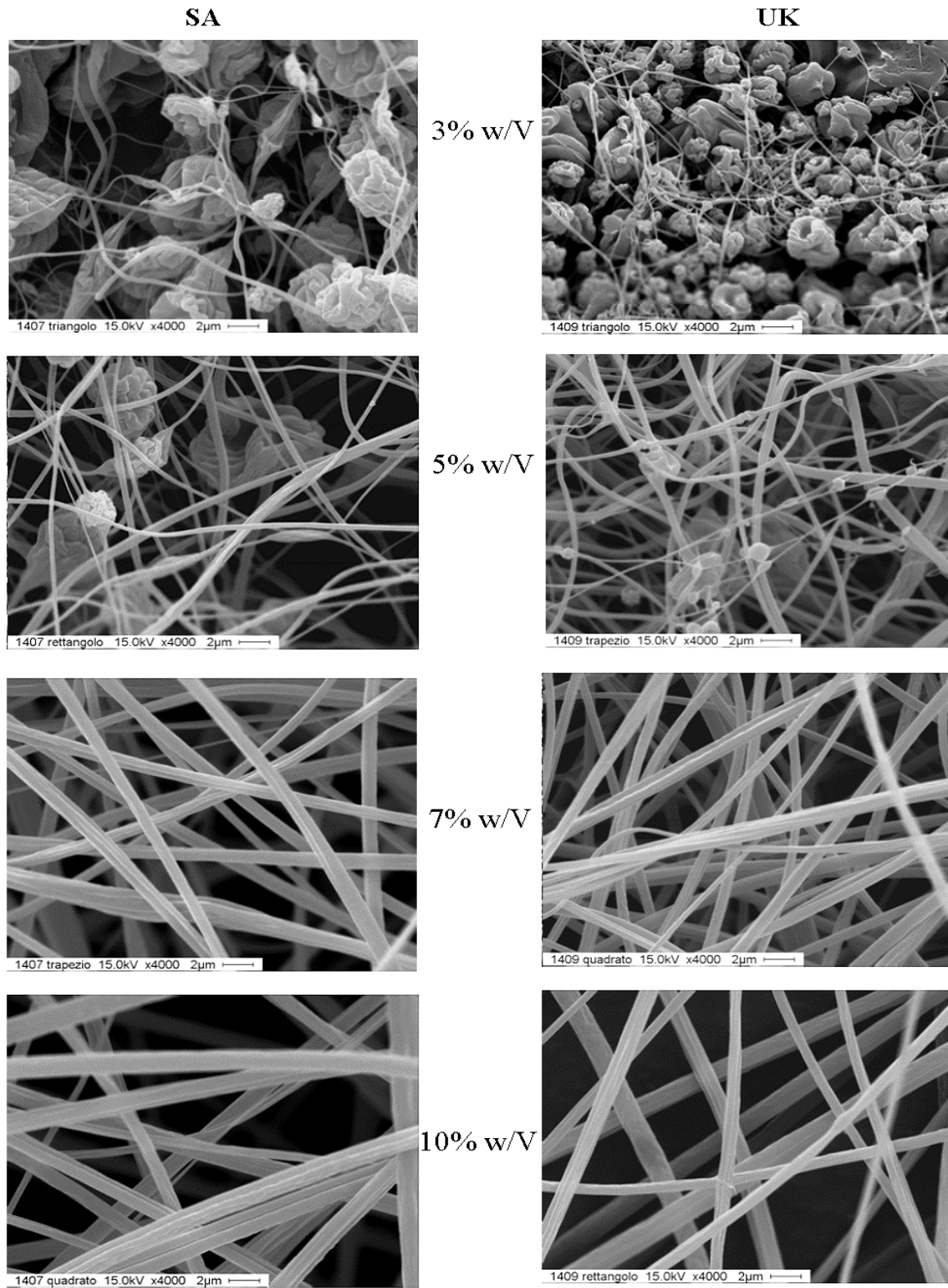
33 for SA, UK and USA respectively. From these expressions knowing the concentration of a solution the time to breakup can be estimated to check its processability.

$$t_b = 2.8 * 10^{-5} c^{3.9} \quad (31)$$

$$t_b = 5.7 * 10^{-5} c^{3.7} \quad (32)$$

$$t_b = 3.6 * 10^{-5} c^{3.8} \quad (33)$$

with the concentration (c) measured in %w/v. using these equations we explain the electro spinnability of cellulose acetate. Appendix 4 shows images of the morphology of the SA and UK systems in varying concentration. The formation of bead-on-string is observed for concentrations 3 and 5% w/v. by using the formula, the time to breakup for a solution of concentration 3% w/v are 2ms and 3ms for SA and UK respectively. Likewise for a 5% w/v we have 15ms and 22ms for SA and UK respectively. These times are too short to sustain a fluid filament for the formation of fibers and therefore quickly break into droplets. In the 3% w/v there is a lot of beads-on-strings formed and as the time increases even in the 5% w/v appreciable fibers could be seen with less beads-on-string morphology. Solutions with higher concentration of 7 and 10% w/v shows good fiber morphology as can be seen in the figures 4.12. The times to breakup are 55ms and 222ms for SA concentration 7 and 10% w/v respectively and 76ms and 286ms respectively for UK. As already stated increase in time to breakup with concentration and therefore extensional viscosity is to reduce the rate of thinning process thereby increasing the time to breakup.



Condition of electrospinning: Distance between needle and target: 15cm, Potential: 15 kV, Flow rate: 0.05ml/min

Figure 4.12 Images of electrospun fiber of SA and UK prepared by Dr. Focarete at the Dept. of Chemistry, “G. Ciamician” Università di Bologna

5.0 conclusion

In this project we have first characterized cellulose acetate from three suppliers and having different molecular weight (M_w) dissolved in a mixture solvent of dichloromethane and methanol (75:25) using an extensional rheometry (CaBER), which seems to be a suitable technique for characterizing materials in extensional flow. From these experiments, the behaviour of these solutions was found to be Newtonian. This has been justified by the very low relaxation times predicted for the solution as compared to the experimental stretching time.

With the aim of ranking the cellulose acetate with respect of their spinnability, the steady state extensional viscosity was determined at several temperatures and concentrations. As a matter of fact, the effect of temperature could not be observed due to concurrent evaporation of the solvent causing a change in concentration during the tests. Conversely, it was possible to observe a power law dependence of the steady state extensional viscosity on concentration. The power law index is higher for UK and USA, and lower for SA. Interestingly if the shear viscosity is considered, the UK and SA display the same power law index which is lower than that determined for extensional viscosity.

A clear correlation was found between these quantities, and as extensional viscosity was correlated with concentration, a correlation between time to breakup and concentration was determined. This is again a power law in the form $t_b = Kc^\alpha$. This power law index (α) is similar for the three materials. The constant (K) however is quite different for the three materials with $K_{UK} > K_{USA} > K_{SA}$

By comparing t_b at different concentration with the results of a series of electrospinning tests on UK and SA solutions, it seems that for t_b higher than 55ms the materials can be electrospun without bead-on-string defects. However, a better understanding of the phenomenon during electrospinning should be studied in further works taking into account at least the effect of evaporation during processing.

6.0 References

- [1] Shelley L. Anna and Gareth H. McKinley, “Elasto-capillary thinning and breakup of model elastic liquids”, *J. Rheology* 45, 115-138 (2001)
- [2] Gareth H. McKinley, and Anubhav Tripathi, “How to extract the Newtonian viscosity from capillary breakup measurements in a filament rheometer”, *J. Rheology* 44, 653-670 (2000)
- [3] C. Clasen, and W. M. Kulicke, “Determination of viscoelastic and rheo-optical material functions of water-soluble cellulose derivatives”, *Prog. Polymer Science* 26, 1839-1919 (2001).
- [4] Howard A. Barnes, “Handbook of elementary Rheology” Cambrian Printers, 2000.
- [5] R.P. Chhabra, “Non-Newtonian Fluids: An Introduction” Department of Chemical Engineering, Indian Institute of Technology, Kanpur
- [6] “Introduction to Rheology” RheoTec messtechnik GmbH.
- [7] Jian H. Yu, Sergey V. Fridrikh, and Gregory C. Rutledge, “The role of elasticity in the formation of electrospun fibers”, *Polymer* 47, 4789-4797 (2006)
- [8] Andreas Greiner, and Joachim H. Wendorff, “Electrospinning: A fascinating method for the preparation of Ultrathin Fibers”, *Angew. Chem. Int. Ed.*, 46, 5670-5703 (2007).
- [9] P. Rustemeyer (Ed), “Cellulose acetate: Properties and Applications”, Wiley-VCH 2004.
- [10] Bhardwaj, Miller, and Rothstein, *J. Rheol.* 514, 693-719 (2007)
- [11] Cambridge Polymer Group
- [12] Steffen Fischer, Katrin Thummler, Bert Volkert, Kay Hettrich, Ingeborg Schmidt, Klaus Fischer “Properties and Application of Cellulose Acetate” *macromol. Symp.* 262, 89-96 (2008)
- [13] J. A. Mitchell and J. C. Umberger, “Viscosity – Concentration Relations of Cellulose Acetate”, *Industrial and Engineering Chemistry*, vol.3 No. 1, 124-128.

- [14] Ani Idris, A. F. Ismail, S. A. Gordeyev, S. J. Shilton, "Rheology Assesment of Cellulose Acetate spinning solution and its influence on the reverse osmosis hollow fiber membrane" polmer testing 22, 319-325 (2003).
- [15] Collins Appaw, Richard D. Gilbert, Saad A. Khan "Viscoelastic Behavior of Cellulose Acetate in a Mixed Solvent System" American Chemical Society, Biomacromolecules Vol. 8, No 5, 1541-1547 (2007).
- [16] Anubhav Tripathi, Stephen H. Spiegelberg, Gareth H. McKinley, "Studying the Extensional Flow and Break up of Complex Fluids using Extensional Rheometers" XIIIth International Congress on Rheology, Cambridge, UK, 2000 (55-57)
- [17] Mette Irene Kolte, Peter Szaboa, "Capillary Thinning of Polymeric Filaments" J. Rheol. 43(3), 601-625 (1999).
- [18] A. V. Bazilevskii², V. M. Entov, A. N. Rozhkov, "Breakup of an Oldroyd Liquid Bridge as a Method for Testing the Rheological Properties of Polymer Solutions" Polymer Science, Series A Vol. 43 No. 7, 716-726 (2001)
- [19] M. Wang, G.C. Rutledge, Alex J. Hsieh, "Electrospinning of Poly (MMA-CO-MAA) Copolymers and their layered Silicate Nanocomposites for Improved thermal Properties", (2004)
- [20] Lucy E. Rodd, Timothy P. Scott, Justin J. Cooper-White, Gareth H. McKinley, "Capillary Break-up Rheometry of Low-Viscosity Elastic Fluids" Applied Rheology, Vol. 15, 12-27 (2005).
- [21] Liang Chen, Lev Bromberg, T. Alan Hatton, Gregory C. Rutledge "Electrospun Cellulose Acetate Fibers containing Chlorhexidine as a bactericide" Polymer 49, 1266-1275 (2008).
- [22] Ji-Huan He, Yu-Qin Wan, Jian-Yong Yu "Effect of Concentration on Electrospun Polyacrylonitrile (PAN) Nanofibers" Fibers and Polymers 2008, Vol.9, No.2, 140-142 (2008)
- [23] Raniero Mendichi, "Caratterizzazione Molecolare Acetato di cellulosa" Laboratorio di Caratterizzazione Molecolare e Reologica, Istituto per Lo Studio Della Macromolecole, 2010.

- [24] Davide Colombo “Comportamento reologico di soluzioni diacetato di cellulose” Tesi di Laurea, Politecnico di Milano (2009/2010)
- [25] W. K. Wee, M. R. Mackley “Rheology and processing of a concentrated cellulose acetate solution” Chemical Engineering Science, vol. 53, No. 6, pp. 1131 – 1144 (1998)
- [26] Abdel-Azim A. Abdel-Azim, Aiman M. Atta, Medhat S. Farahat, Wagdy Y. Boutros “Determination of intrinsic viscosity of polymeric compounds through a single specific viscosity measurement” Polymer Vol. 39 No. 26, 6827-6833 (1998)
- [25] Christian Clasen, J.P. Plog, W.-M. Kulicke, M. Owens, C. Macosko L.E. Scriven, M. Verani, Gareth H. McKinley “How Dilute are Dilute solutions in Extensional flows?” Hatsopoulos Microfluids Laboratory, Dept. of Mechanical Engineering, Massachusetts Institute of Technology, Report No. 06-P-09. (2006)

7.0 Appendix

7.1 Appendix 1

Normalised Diameter vs Time, 7% wt/v

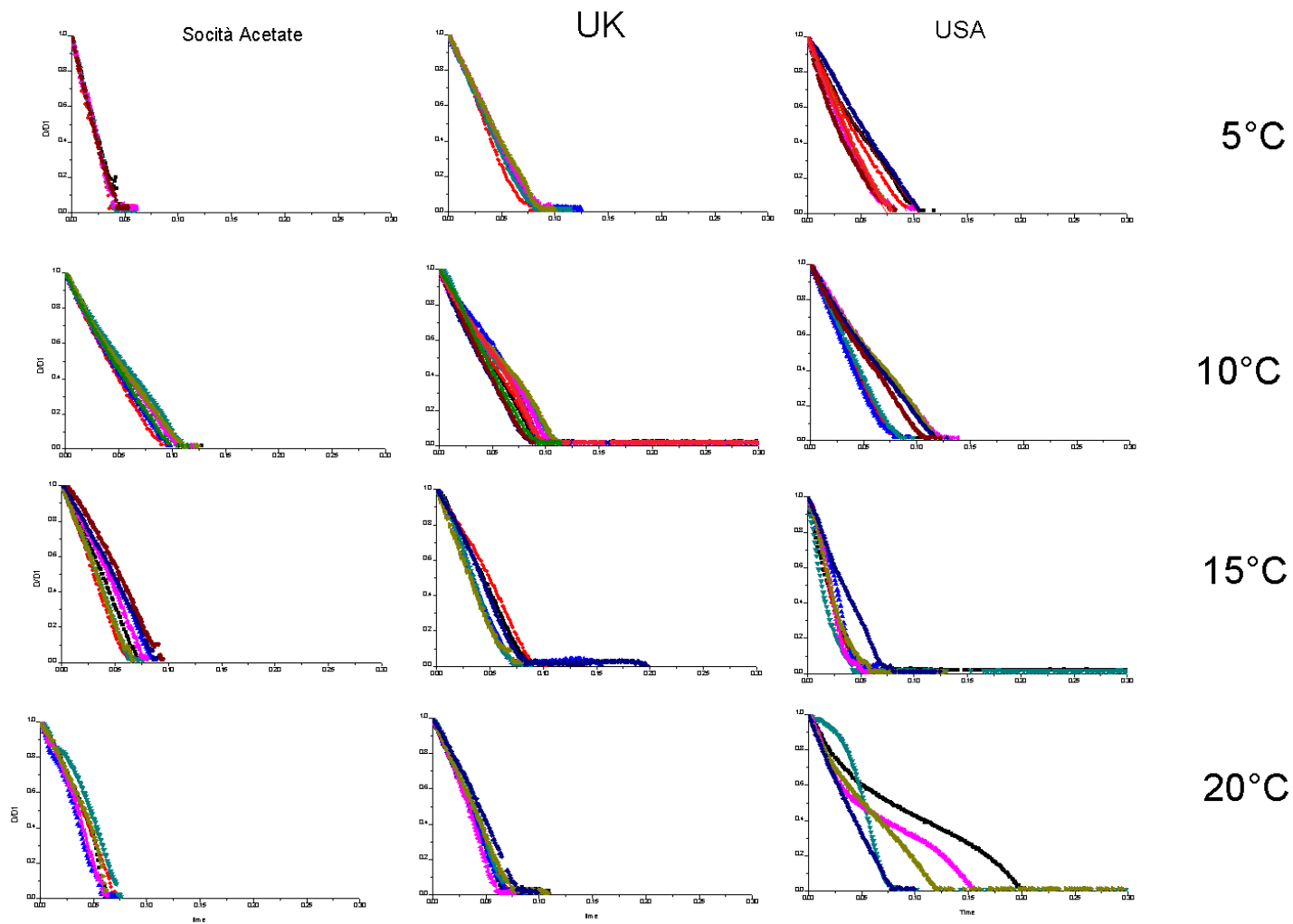


Figure 7.1 Normalised Diameter vs. Time for 7% w/v

Normalised Diameter vs Time 10% wt/v

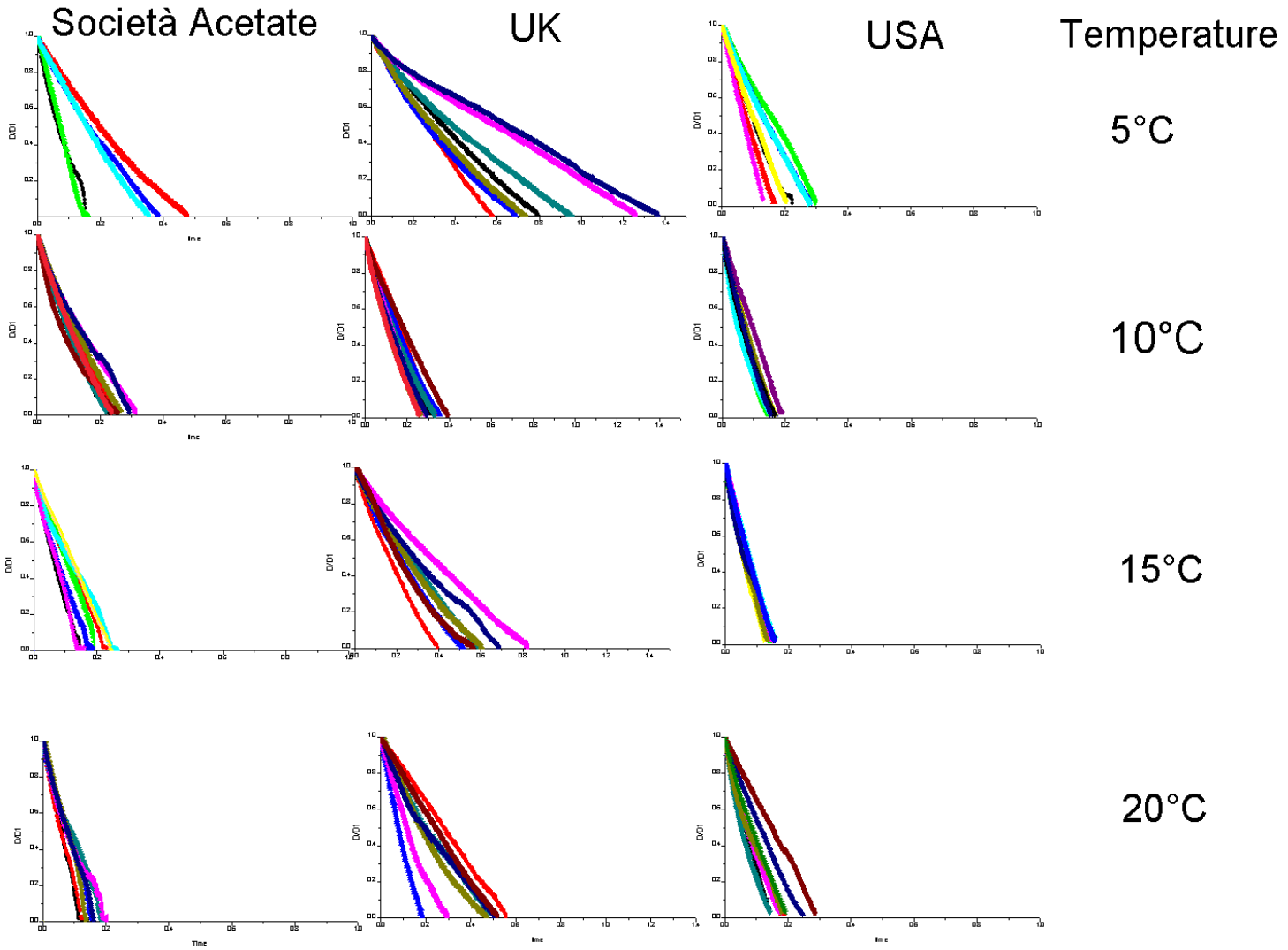


Figure 7.2 Normalised Diameter vs. time for 10% w/v

Normalised Diameter vs Time 12.5% wt/v

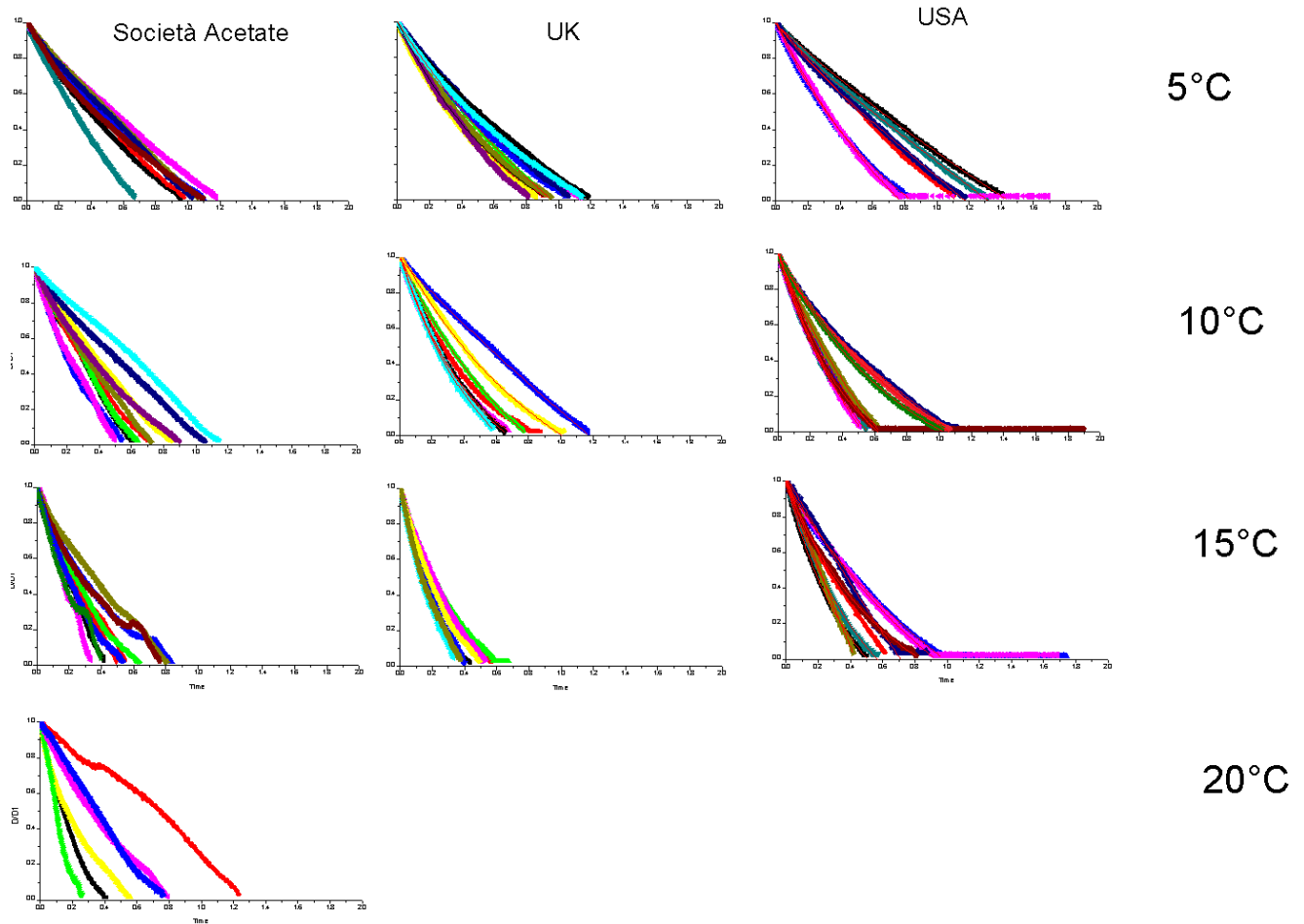


Figure 7.3 Normalised diameter vs. time for 12.5% w/v

7.2 Appendix 2

Apparent Extensional viscosity vs. Hencky strain (7% w/v)

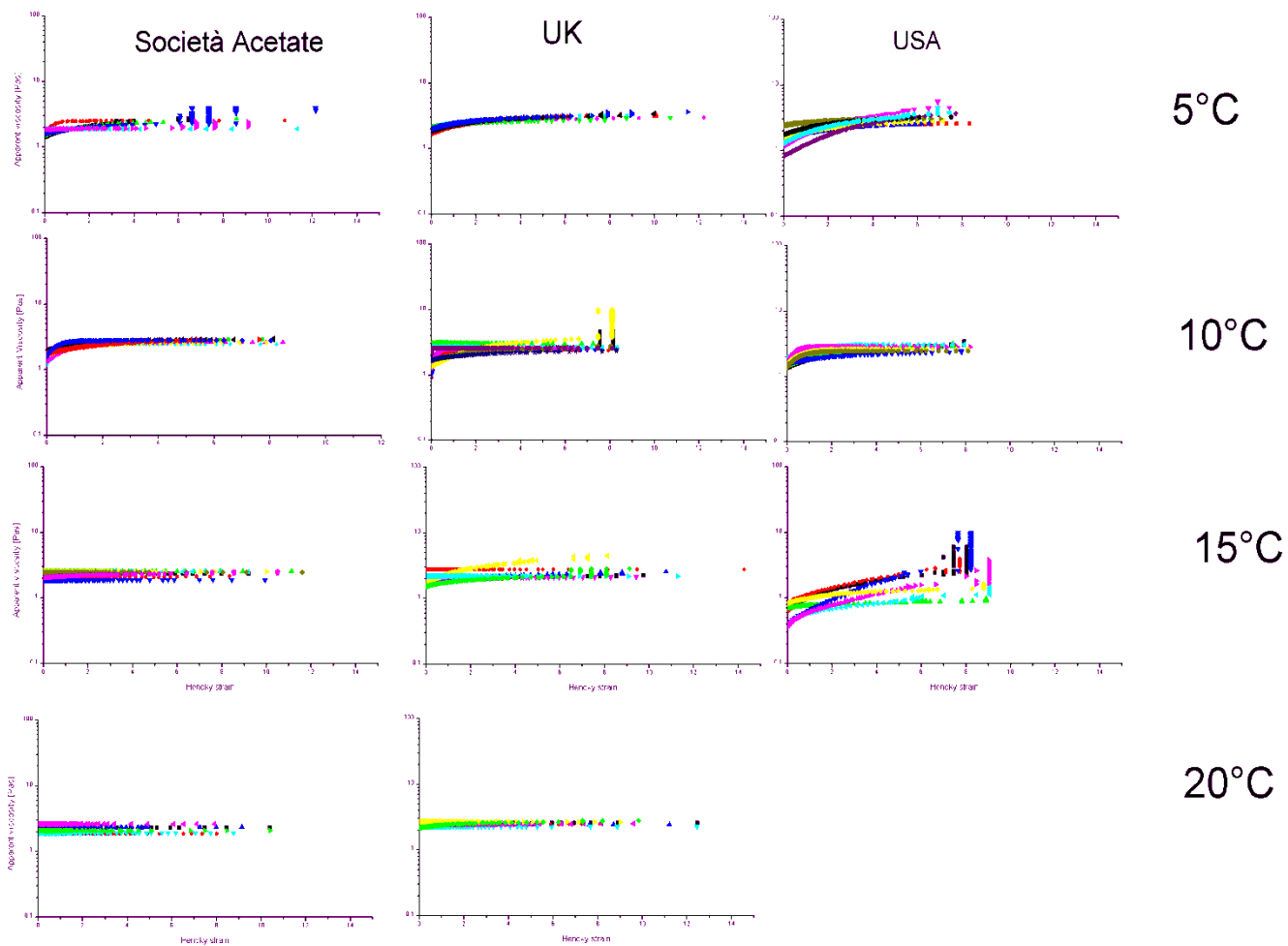


Figure 7.4 Apparent Experiment viscosity vs. Hencky strain 7% w/v

Apparent Extensional Viscosity vs. Hencky Strain (10% w/v)

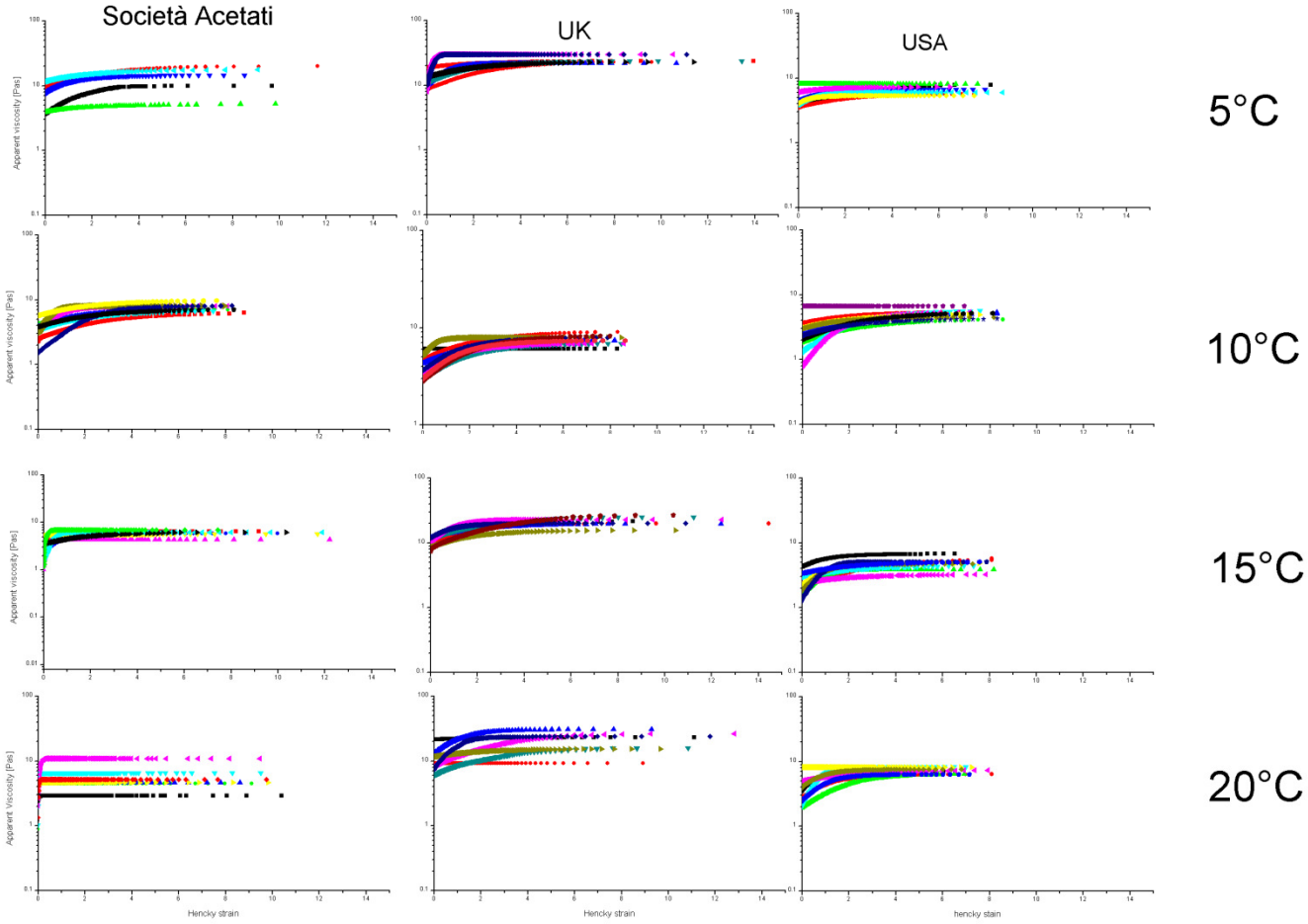


Figure 7.5 Apparent Experiment viscosity vs. Hencky strain 10% w/v

Apparent Extensional Viscosity vs. Hencky Strain (12.5%w/v)

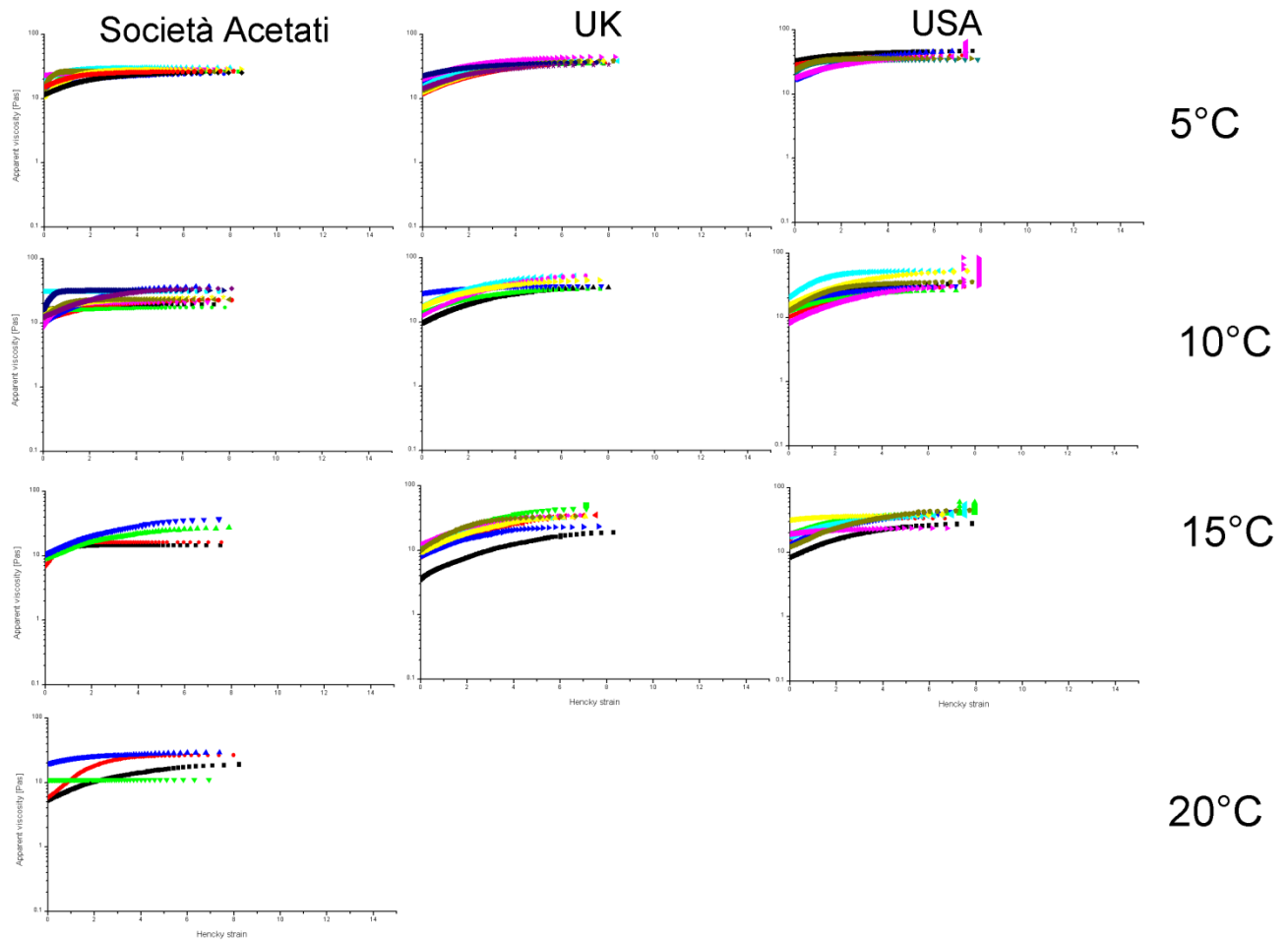


Figure 7.6 Apparent Experiment viscosity vs. Hencky strain 12.5% w/v

7.3 Appendix 3

Societa Acetate	Viscosity [%]			Time to Break up [%]		
	7	10	12.5	7	10	12.5
Temperature Effect						
5°C-10°C	+21	-45	-20	+125	-35	-33
10°C-15°C	-16	-20	+11	-22	-27	-22
15°C-20°C	-4	-3	-11	0	-21	-4

Table 7.1 Relative change in steady state extensional viscosity and time to breakup with temperature for SA

Società Acetate	Viscosity [%]				Time to Break up [%]			
Concentration Effect	5°C	10°C	15°C	20°C	5°C	10°C	15°C	20°C
7 – 10	+500	+174	+163	+165	+900	+189	+171	+114
10 – 12.5	+101	+190	+302	+269	+150	+158	+174	+233

Table 7.2 Relative change in steady state extensional viscosity and time to breakup with concentration for SA

UK	Viscosity [%]			Time to Break up[%]		
Temperature Effect	7	10	12.5	7	10	12.5
5°C-10°C	-10	+10	+12	+11	+9	-11
10°C-15°C	-8	-40	-25	-20	-51	-48
15°C-20°C	+2	24		-13	-44	

Table 7.3 Relative change in steady state extensional viscosity and time to breakup with temperature for UK

UK	Viscosity [%]				Time to Break up [%]			
Concentration Effect	5°C	10°C	15°C	20°C	5°C	10°C	15°C	20°C
7 – 10	+275	+357	+198	+122	+422	+410	+213	+100
10 – 12.5	+238	+244	+333	-	+133	+75	+84	

Table 7.4 Relative change in steady state extensional viscosity and time to breakup with concentration for UK

USA	Viscosity [%]			Time to Break up [%]		
	7	10	12.5	7	10	12.5
Temperature Effect						
5°C-10°C	-10	-24	-9	+11	-23	-33
10°C-15°C	-34	-6	-2	-50	-18	-10
15°C-20°C		+ 50			+36	

Table 7.5 Relative change in steady state extensional viscosity and time to breakup with temperature for USA

USA	Viscosity [%]				Time to Break up [%]			
	5°C	10°C	15°C	20°C	5°C	10°C	15°C	20°C
Concentration Effect								
7 – 10	+116	+84	+163		+144	+70	+180	
10 – 12.5	+499	+618	+643		+400	+335	+379	

Table 7.6 Relative change in steady state extensional viscosity and time to breakup with concentration for USA

7.4 Appendix 4

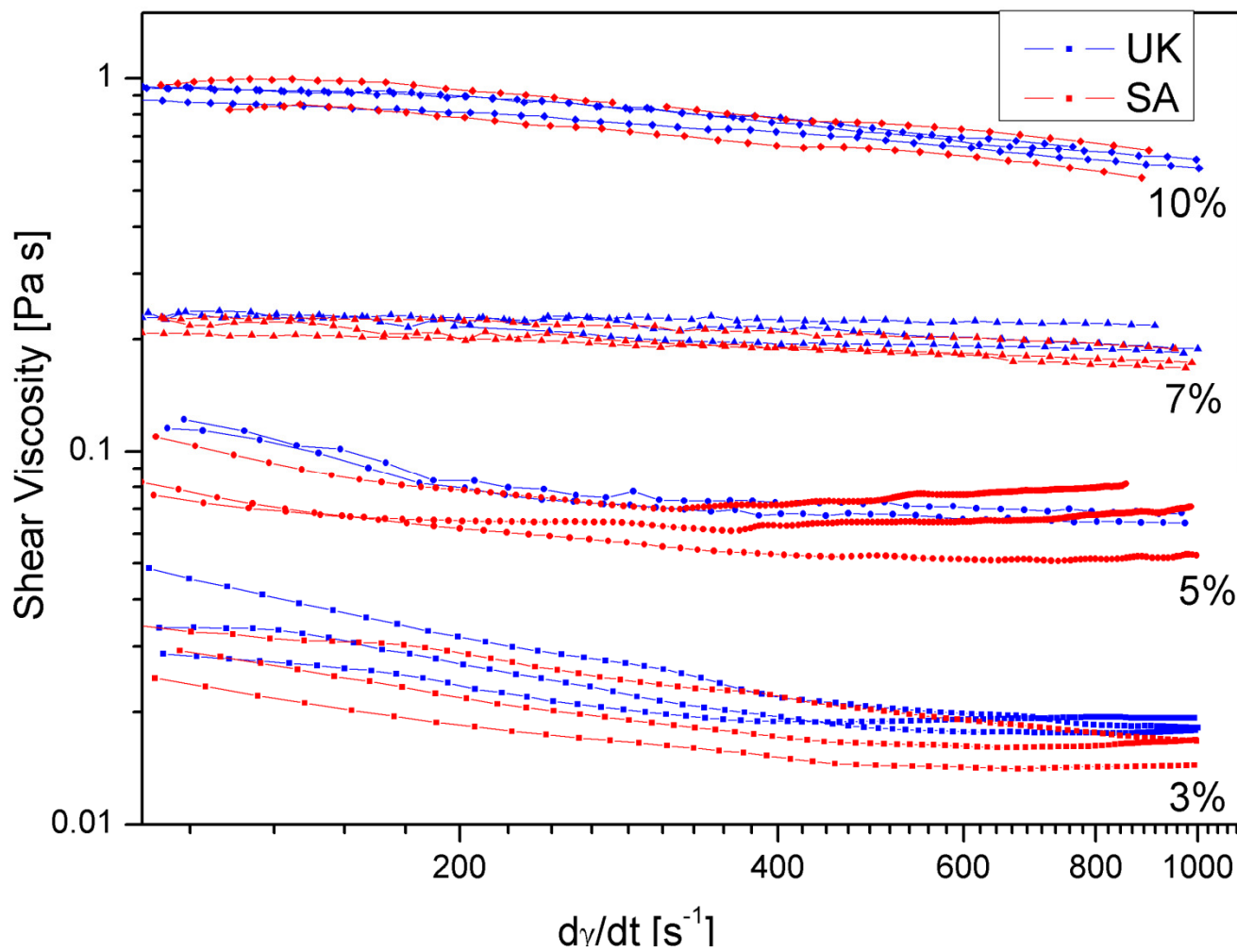


Figure 7.7 Shear viscosities vs. strain rate for SA and UK